Mapping Changes in the Human Cortex throughout the Span of Life

ELIZABETH R. SOWELL, PAUL M. THOMPSON, and ARTHUR W. TOGA
David Geffen School of Medicine
Laboratory of Neuro Imaging, Department of Neurology
University of California, Los Angeles

In this review, the authors summarize the literature on brain morphological changes that occur throughout the human life span from childhood into old age. They examine changes observed postmortem and in vivo where various brain MRI analytic methods have been applied. They evaluate brain changes observed with volumetric image analytic methods and voxel-based morphometric methods that may be used to better localize where changes occur. The primary focus of the review is on recent studies using state-of-the-art cortical pattern-matching techniques to assess age-related changes in cortical asymmetries, gray matter distribution, and brain growth across various age spans. The authors attempt to integrate findings from the in vivo studies with results from postmortem studies and analyze the complicated question of when brain maturation stops and brain aging begins. Analyzing the regional patterns of change initiated at various ages may help elucidate relationships between changing brain morphology and changing cognitive functions that occur throughout life. Long-range longitudinal studies, correlations between imaging and postmortem data, and more advanced image acquisition and analysis technologies will be needed to fully interpret brain morphological changes observed in vivo in relation to development and aging. NEUROSCIENTIST 10(4):372–392, 2004. DOI: 10.1177/1073858404263960

Understanding normative changes in brain structure through the various stages of development and aging is paramount to understanding cognitive changes throughout the human life span. Considerable progress has been made in these endeavors during the past few decades, given the availability of noninvasive imaging tools such as MRI. This revolutionary technological advance allows us to study normally developing and aging individuals because it is not harmful, and thus, it is ethically employed, even in children. Furthermore, it provides the unprecedented opportunity to study individuals at multiple time points. Prior to the advent of these powerful imaging tools, researchers were confined to infer brain changes from postmortem data. Of obvious concern with the postmortem studies is the normalcy of the participants studied after death and the notable scarcity of samples from the younger years of life. Regardless, results from the few existing postmortem studies of cellular changes over various age spans are indispensable for interpreting results from the in vivo imaging studies. With most existing imaging techniques, we observe changes in MR signal values in brain tissue that are only indirectly linked to the cellular makeup that comprises the brain at any given point in time.

A detailed description of the nature of the MR signal and what cellular constituents it represents is beyond the scope of this review. Essentially, however, the source of the MRI signal in all of the structural imaging studies described in this review is associated with water, which is more prominent in the cell bodies of the gray matter, and fat, which is more prominent in the myelin sheath comprising white matter. Changes in the amount of water and/or fat within regional brain tissues that occur with age are the primary source of age effects we observe in studies of brain maturation and in studies of degenerative changes that occur with normal aging when MRI is used. As the reader will see in the following sections, the nature of change in MR signal and the underlying changes in cellular structure are critical to understanding when "maturation" stops and "aging" begins.

In addition to advancement in image acquisition devices, computer technology and software development have also advanced, producing more sophisticated methods for analyzing brain image data. Before quantitative

Address correspondence to: Elizabeth R. Sowell, PhD, University of California, Los Angeles, Laboratory of Neuro Imaging, 710 Westwood Plaza, Room 4-238, Los Angeles, CA 90095-1769 (e-mail: esowell @loni.ucla.edu).

computerized algorithms were used to analyze change in brain structure, MR image data was studied more qualitatively, with attempts to visually discriminate between subjects of various ages based on prominent characteristics such as sulcal depth, signal hyperintensities, or ventricular size. These methods were used typically in older patients (e.g., Kertesz and others 1998) and not to our knowledge in normally developing children. The first quantitative MRI studies in children measured T1 and T2 relaxation times using various imaging protocols (e.g., Holland and others 1986; Hassink and others 1992), providing information regarding the relative signal values and appearance of different brain structures at different ages. Next in the progression of technological advancement in quantitative morphometry came volumetric studies in which tissue segmentation was used to assess total volumes of gray matter, white matter, and cerebrospinal fluid (Jernigan, Archibald, and others 1991; Pfefferbaum and others 1994; Blatter and others 1995). More recently, volumetric studies have assessed localized changes by defining regions of interest within MR data sets on a slice-by-slice basis (Giedd, Vaituzis, and others 1996; Bartzokis and others 2001; Jernigan and others 2001; Sowell, Trauner, and others 2002). These methods are considered a gold standard for regional volume assessment (to the extent that regional cortical definition is valid and reliable) because they are not dependent on image averaging across subjects, which can require brain images to be spatially distorted and may inaccurately match anatomy across subjects.

The main focus of this review will be on the exciting new studies of normative brain development and aging that have been accomplished with state-of-the-art brain-mapping techniques. These studies have allowed us to map structural changes over the entire cortical surface and have considerably advanced our understanding of the timing and localization of these alterations that occur as part of the sculpting of the human brain at various ages. Mapping techniques, such as voxel-based morphometry (VBM) and cortical pattern matching, provide an advantage over the more traditional volumetric studies because they can visualize changes occurring within the brain and at the cortical surface, unbiased by observable sulcal cortical boundaries necessary for making anatomical delineations in the volumetric studies. In the following paragraphs, we will describe cellular changes observed in the postmortem literatures on development and aging that likely underlie the changes we observe with MRI. We will then describe changes in brain structure observed in brain-mapping studies of children and adolescents and move ahead in time (with increasing age) to describe structural changes observed in aging populations. Then we will attempt to integrate these postmortem and in vivo literatures in the hope of furthering our understanding of distinctions between development and aging. This review will focus on changes that occur in the cerebral cortex because these have been the focus of the most recent, cutting-edge brain-mapping studies.

Postmortem Studies

Maturation

From postmortem studies, we know that myelination begins near the end of the second trimester of fetal development and extends beyond the second decade of life (Yakovlev and Lecours 1967). Autopsy studies consistently reveal that myelination occurs in a systematic sequence with different brain regions myelinating at different times. Generally, myelination is thought to progress from inferior to superior brain regions and from posterior to anterior; that is, brain stem and cerebellar regions myelinate prior to the cerebral hemispheres, and the occipital lobes myelinate prior to the frontal lobes (Yakovlev and Lecours 1967; Brody and others 1987). This process is thought to reflect the regional pattern of functional maturation of the brain.

More recently, Benes and colleagues (1994) examined the brains of 164 subjects from 0 to 76 years of age, including many subjects in the peripubertal age range. Specifically, they studied the extent of myelination along the surface of the hippocampal formation at the level of the subiculum, presubiculum, and parasubiculum (referred to as the superior medullary lamina) using a computer-assisted quantitative technique. Benes and colleagues found a 95% increase in the area of myelination of the superior medullary lamina in the first and second decades of life. Notably, when the authors corrected their measure for overall changes in cerebral size (e.g., area of myelination expressed relative to brain weight), they still found a 92% area increase between groups of subjects aged 0 to 9 and 10 to 19 years. They describe in detail the known connectivity of the subicular and presubicular regions, indicating that at least some of the axons myelinating in this region in adulthood could originate from the cingulate gyrus. Thus, Benes and colleagues speculate that the functional significance of the increased myelination that they observe could be related to corticolimbic integration thought to be involved in the regulation of emotional behaviors with greater cognitive maturity.

In addition to continuing myelination during childhood and adolescence, a regionally variable reduction in synaptic density also occurs (Huttenlocher 1979; Huttenlocher and de Courten 1987). The relationship between findings in postmortem studies and findings from in vivo studies is not yet clear. Although continuing myelination and reductions in synaptic density are known to occur throughout adolescence, which factors contribute most to gross morphological changes observable with neuroimaging are not known. As discussed in detail by Giedd, Snell, and colleagues (1996), reductions in synaptic density are not likely to account for the large-volume decreases in gray matter structures observed in vivo throughout adolescence (Jernigan, Trauner, and others 1991; Caviness and others 1996; Reiss and others 1996; Sowell, Trauner, and others 2002). Rather, it seems more likely that changes in myelination account

for overall brain size changes. Cell-packing density and somal size can also account for structure size. These variables are influenced by hydration levels, degree of vascularity, hormones, and nutrition (Giedd, Snell, and others 1996). Postmortem studies of total brain weight have consistently shown dramatic increases during the first 5 or 10 years of life but less dramatic increases into the late teens and early 20s. This brain growth is followed by a gradual decline beginning at about 45 or 50 years of age (Dekaban 1978; Ho and others 1980). The question of whether myelination or synaptic pruning is more responsible for changes in brain size or cortical gray and white matter distributions may partly be answered by findings from recent brain-mapping studies described below.

Aging

As mentioned above, postmortem studies show that total brain weight is relatively stable between the 20s and late 50s in humans and then gradually declines. The same studies show that loss in total brain weight may be more marked in the eighth decade and beyond (Dekaban 1978; Ho and others 1980). Myelination continues in some brain regions well into the fifth decade (Benes and others 1994) and perhaps even beyond into senescence (Yakovlev and Lecours 1967). At the same time, the total length of myelinated fibers declines significantly between the ages of 20 and 80 years, reflective of small but not large nerve fiber loss (Marner and others 2003). However, in the same postmortem sample, neocortical neuron density remained relatively stable (Pakkenberg and Gundersen 1997). This may be because the fibers lost are small collaterals rather than the main axon, which would explain the loss of neuronal fibers in the absence of a comparable loss of neuronal density (Pakkenberg and Gundersen 1997; Marner and others 2003). As noted almost a decade earlier (Terry and others 1987), neuronal shrinkage, rather than cell loss, accounts for the cortical volume loss observed during the normal aging process. Regionally, the age-related changes in neuronal size appear most prominent in frontal and temporal lobes, with less dramatic changes in the parietal cortices.

Summary of Postmortem Findings

As should be clear from the brief review above, myelination and synaptic pruning predominate changes in the cortical neuropil during childhood and adolescence, and during aging, loss of axonal fibers and neuronal shrinkage predominate. However, the overlap in the age range between developmental changes and changes that are more specific to aging is considerable. There is no clear pattern from these postmortem studies to time lock the progressive changes from the regressive, degenerative changes that occur during aging. Clearly, new and improving cognitive abilities such as language acquisition, reading, fine motor skills, and problem solving are a hallmark feature of human maturation, whereas some,

but perhaps not all, of these skills begin to decline as the aging process continues. Thus, there must be a distinction between maturational and degenerative processes, and examination of these questions using in vivo MRI is the focus of the remainder of this review.

In Vivo Studies

Volumetric Image Analysis Findings

Maturation

Numerous volumetric MRI studies have focused on brain developmental changes that occur during childhood and adolescence (Jernigan, Trauner, and others 1991; Pfefferbaum and others 1994; Caviness and others 1996; Giedd, Snell, and others 1996; Giedd, Vaituzis, and others 1996; Reiss and others 1996; Sowell and Jernigan 1998; Giedd and others 1999; Courchesne and others 2000; Sowell, Trauner, and others 2002). The volumetric studies to date have used various methods to assess age effects on volume in various brain regions and tissues. Tissue segmentation has been employed to assess gray matter, white matter, and CSF differences with age. Earlier studies in the literature tended to use stereotaxic region definition schemes (Jernigan, Trauner, and others 1991; Giedd, Snell, and others 1996; Reiss and others 1996), frequently because the image spatial resolution was low (i.e., 4 to 5 mm slice thickness) relative to more recent studies in which high-resolution T1-weighted image volumes are assessed (i.e., 1 to 1.5 mm slice thickness). In some of these studies, whole brain tissue volumes were assessed for age effects (Caviness and others 1996; Courchesne and others 2000), and others have employed manual region definition on a slice-by-slice basis using cortical anatomical landmarks (where observable) as boundaries (Giedd, Vaituzis, and others 1996; Lange and others 1997; Sowell and Jernigan 1998; Sowell, Trauner, and others 2002). Finally, automated lobar region definition schemes have been used (Giedd and others 1999), in which image-warping algorithms are used to map standardized lobar measures to each individual subject's brain.

Regional differences in the processes (e.g., myelination, synaptic pruning) that result in cortical gray and white matter volume changes observed with MRI would be expected given postmortem findings of regional differences in the timing of progressive and regressive events in brain maturation. In the earliest report of volumetric findings between childhood and young adulthood, Jernigan and Tallal (1990) reported that children aged 8 to 10 years had significantly more cortical gray matter relative to cerebral size than did young adults. In a subsequent report in which more subjects were studied and cortical and subcortical gray matter structures were subdivided (cortical regions defined stereotaxically), Jernigan, Trauner, and others (1991) found evidence for

an increase in size of the superior cranial vault, particularly in the anterior region. Within the superior cranial vault, the cortical gray matter appeared to be decreasing with age whereas CSF in this region increased. The inferior cortical gray matter volumes did not appear to change across the age range. The authors proposed that their observation of a thinning cortex in superior cortical regions could be related to the processes that led to the earlier reported reductions in synaptic density. Since these early reports, cortical gray matter volume decreases were reported by other groups (Pfefferbaum and others 1994; Reiss and others 1996). Regionally, the most notable changes during childhood and adolescence occur in the more dorsal cortices. During adolescence, frontal and parietal lobes show highly significant increases in white matter along with concomitant decreases in gray matter (Giedd and others 1999; Sowell, Trauner, and others 2002). The more ventral cortices of the temporal lobes change less dramatically between childhood and adolescence (Jernigan, Trauner, and others 1991; Giedd and others 1999; Sowell, Trauner, and others 2002). Notably, gray matter thinning in the frontal cortex is related to changing cognitive ability in normal children and adolescents. We found significant correlations between gray matter volume in the frontal lobe and children's performance on a verbal learning task (Sowell, Delis, and others 2001).

Aging

Volumetric imaging studies in adult aging populations have been very enlightening and are, again, a gold standard in beginning to understand the effects of increasing age on brain tissue. Consistent in most studies are findings of gray matter volume loss with age (Jernigan, Archibald, and others 1991; Pfefferbaum and others 1994; Blatter and others 1995; Courchesne and others 2000; Bartzokis and others 2001; Ge and others 2002; Bartzokis and others 2003). White matter volume loss has also been consistently reported in these cross-sectional samples (Jernigan, Archibald, and others 1991; Pfefferbaum and others 1994; Blatter and others 1995; Courchesne and others 2000; Bartzokis and others 2001; Ge and others 2002; Bartzokis and others 2003). Regionally, gray matter loss appears more prominent in the frontal cortex than in other lateral cortical regions (Raz and others 1997; Bartzokis and others 2001; Jernigan and others 2001) and may be more specific to nonorbital frontal regions (Salat and others 2001). White matter loss may be more prominent than gray matter loss (Jernigan and others 2001), but this depends on the starting age ranges in the cross-sectional samples studied. This is because white matter changes in adulthood appear nonlinear, with white matter gain continuing into approximately the mid-40s, followed by more prominent loss (Bartzokis and others 2001; Ge and others 2002; Sowell and others 2003). Again, frontal white matter volumetric changes during aging appear more prominent than those in other regions, such as the temporal lobes

(Bartzokis and others 2001; Jernigan and others 2001). From the cross-sectional studies, age-related loss of brain tissue can only be inferred, given that the same individuals were not studied at multiple time points. Recent longitudinal analyses in normative aging populations conducted by Resnick and colleagues (2000) have yielded promising results. The only significant longitudinal findings after 1 year were of ventricular size increase, probably because the interscan interval was relatively short. At 2- and 4-year follow-up, however, tissue loss was highly significant within individuals (5.4% total brain volume loss) and was more prominent in frontal and parietal cortices than for temporal and occipital cortices. These findings are generally consistent with the cross-sectional results.

Mapping with VBM

Maturation

The question of spatial localization of maturational changes cannot be fully addressed with volumetric methods in which, typically, only gross lobar structures can be reliably visually identified and manually defined. Newer methods, initially used to evaluate functional imaging data, have been employed to assess structural effects during normal development on a voxel-by-voxel basis (Paus and others 1999; Sowell, Thompson, Holmes, Batth, and others 1999; Sowell, Thompson, Holmes, Jernigan, and others 1999). We used VBM (Ashburner and Friston 2000) to localize age-related gray matter density reductions between childhood and adolescence in 18 normally developing individuals between 7 and 16 years of age (Sowell, Thompson, Holmes, Batth, and others 1999). Essentially, VBM entails automated spatial normalization of volumes into a standard coordinate space and scaling of images so that each voxel coordinate is anatomically comparable across subjects. Tissue segmentation and spatial smoothing is then used to assess localized differences in gray matter and/or white matter. Results from these analyses revealed that the gray matter volume reductions observed in frontal and parietal lobes in the volumetric studies of brain maturation resulted mostly from gray matter density reductions in diffuse dorsal regions of these cortices (Sowell, Thompson, Holmes, Batth, and others 1999). The parietal cortex changed the most in both the volumetric and VBM assessments of gray matter, and relatively little change occurred in the more ventral cortices of the temporal and occipital lobes in these normally developing children and adolescents (see Fig. 1). In a similar study, Paus and colleagues (1999) used VBM to assess white matter changes in subjects 4 to 17 years of age and found prominent white matter density increases in the posterior limb of the internal capsule and in the arcuate fasciculus in the temporo-parietal region. The prominent findings in the parietal cortex, relative to the frontal cortex, were not expected, given

the known posterior to anterior progression of maturational cellular events. We fully expected frontal maturation to have been well under way by age 17 and reflected in the VBM results.

We decided to test the hypotheses that frontal gray matter changes must occur later in adolescence by conducting a VBM study focusing on the adolescent to adult age range. As described above, between childhood and adolescence, cortical changes were diffusely distributed in dorsal frontal and parietal regions (Sowell, Thompson, Holmes, Batth, and others 1999). In striking contrast, however, the pattern of cortical maturation between adolescence and adulthood was localized to large regions of dorsal, mesial, and orbital frontal cortex with relatively little gray matter density reduction in the parietal lobes or in any other cortical region (Sowell, Thompson, Holmes, Jernigan, and others 1999) (see Fig. 1). These results make sense in light of studies showing that the frontal lobes are essential for such functions as response inhibition, emotional regulation, planning, and organization (Fuster 1997), which may not be fully developed in adolescents.

Aging

To our knowledge, only one study has used VBM to assess age effects in normal adults (Good and others 2001). In this study, 465 normal individuals between 17 and 79 years of age were assessed. Global gray matter volume significantly declined with age, and regional patterns suggested that above and beyond the global gray matter loss, gray matter density reduction occurred in regions including bilateral superior parietal regions, pre- and postcentral gyri, insula/frontal operculum right cerebellum, and anterior cingulate. Accelerated loss was also noted in the left inferior frontal gyrus and in some temporal lobe regions. Generally, these results are consistent with the volumetric studies in which parietal and frontal regions may have more prominent gray matter volume loss with aging. Good and colleagues (2001) noted trends for nonlinear age effects in global white matter volume, and regionally, cortical white matter loss was most prominent in frontal and occipital regions. Other studies have shown more prominent white matter loss (Courchesne and others 2000; Bartzokis and others 2001; Jernigan and others 2001; Sowell and others 2003), but the oldest subjects studied by Good and colleagues were underrepresented relative to the other studies. Taken together, these studies suggest that white matter volume loss accelerates in the eighth and ninth decades relative to the sixth and seventh.

Cortical Pattern Matching

Although the VBM approach has clear advantages over the volumetric studies in which only gross lobar regions are assessed, there are also disadvantages related to more technical aspects of image averaging. The problem with VBM is that typically, automated image registration
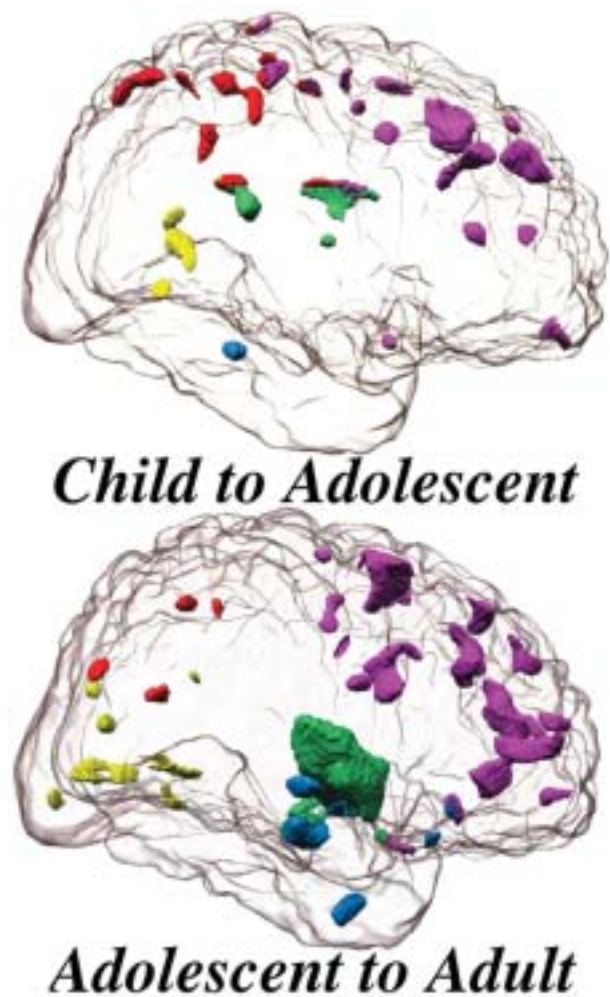

Fig. 1. *Top*, Child minus adolescent statistical map for the negative age effects representing gray matter density reductions observed between childhood and adolescence. *Bottom*, Adolescence and adulthood. These maps are three-dimensional renderings of the traditional statistical maps shown inside the transparent cortical surface rendering of one representative subject's brain. Lobes and the subcortical region were defined anatomically on the same subject's brain. Color coding is applied to each cluster based on its location within the representative brain. Clusters are shown in the frontal lobes (purple), parietal lobes (red), occipital lobes (yellow), temporal lobes (blue), and subcortical region (green) (Sowell, Thompson, Holmes, Batth, and others 1999; Sowell, Thompson, Holmes, Jernigan, and others 1999).

techniques are used to spatially normalize brain volumes across subjects. Considerable variability exists in regional sulcal patterns across individuals, with variability more pronounced the further the region is from the center of the brain. The variability in sulcal patterns also differs by cortical region. Recent brain-mapping studies have shown cortical variability of 10 to 20 mm, particularly in the posterior temporal lobe regions in children (Sowell, Thompson, Rex, and others 2002), adults (Narr and others 2001), and the aged (Thompson and others

1998), even after spatial normalization (see Fig. 2, variability). Thus, when brain volume data sets are normalized without taking this variability into account, cortical anatomical regions are not likely well matched across subjects, particularly where sulcal pattern variability is highest. The same methods that allow us to assess cortical variability can be used to assess group differences in gray matter density while accounting for the differences in sulcal location across subjects.

Cortical pattern–matching methods allow us to match cortical anatomy across subjects and account for the interindividual differences in cortical patterns. They can be used to encode both gyral patterning (as shown in Fig. 2) and gray matter variation. This may substantially improve the statistical power to localize age-related changes, relative to the VBM studies described above. These cortical analyses discriminate the effects of gyral shape variation from gray matter change, and they can also be used to measure cortical asymmetries (Thompson and others 1998; Sowell, Thompson, Rex, and others 2002). Briefly, a three-dimensional geometric model of the cortical surface is extracted from the MRI scan (MacDonald and others 1994) and then flattened to a two-dimensional planar format (Thompson and Toga 1997, 2002). A complex deformation, or warping transform, is then applied that aligns the sulcal anatomy of each subject with an average sulcal pattern derived for the group (see Fig. 3). To improve sulcal alignment across subjects, all sulci that occur consistently can be manually defined on the surface rendering (see Fig. 4) and used to restrict this transformation. Cortical pattern matching adjusts for differences in cortical patterning and shape across subjects. Cortical measures, such as gray matter thickness or local brain size, can then be compared across subjects and groups. Sulcal landmarks are used as anchors, as homologous cortical regions are better aligned after matching sulci than by just averaging data at each point in stereotaxic space, as is done in traditional VBM (Ashburner and Friston 2000). Given that the deformation maps associate cortical locations with the same relation to the primary folding pattern across subjects, a local measurement of gray matter density is made in each subject and averaged across equivalent cortical locations. To quantify local gray matter, we use a measure termed *gray matter density*, used in many prior studies to compare the spatial distribution of gray matter across subjects. This measures the proportion of gray matter in a small region of fixed radius (15 mm) around each cortical point (Sowell, Thompson, and others 2001; Thompson, Mega, Woods, and others 2001; Thompson, Vidal, and others 2001; Sowell, Thompson, Rex, and others 2002). Given the large anatomic variability in some cortical regions, high-dimensional elastic matching of cortical patterns is used to associate measures of gray matter density from homologous cortical regions across subjects (as shown in Fig. 4). One advantage of cortical matching is that it localizes age effects relative to gyral landmarks, as illustrated in elderly sub-
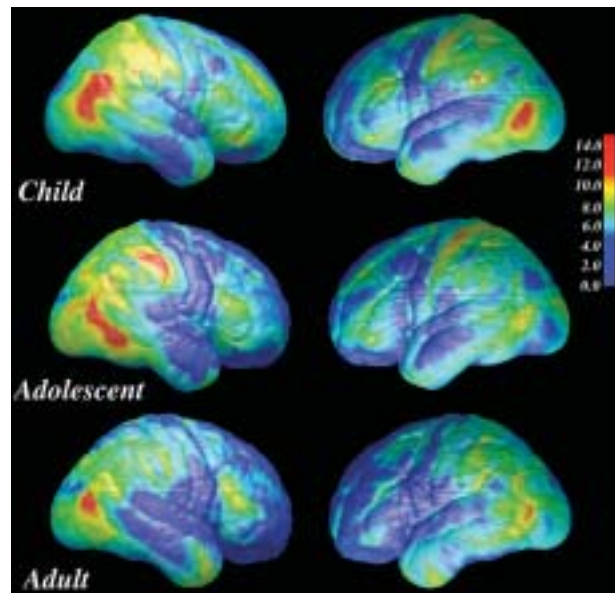

Fig. 2. Cortical surface variability maps in three dimensions viewed from the right and the left showing variability in the average child (*n* = 14), the average adolescent (*n* = 11), and the average young adult (*n* = 10). The color bar indicates patterns of variability within each group as the root mean square magnitude (in mm) of displacement vectors required to map each individual into the group average surface mesh. Note that this map is representative of residual brain shape variability after affine transformation into ICBM305 standard space. Higher variability is observed in the postcentral gyrus and posterior temporal regions in all three age groups, with relatively less variability in precentral and anterior temporal gyri (Sowell, Thompson, Rex, and others 2002).

jects in Figure 5; it also averages data from corresponding gyri, which would be impossible if data were only linearly mapped into stereotaxic space. The effects of age, gender, medication, disease, and other measures on gray matter can be assessed at each cortical point.

Maturation

Using cortical pattern–matching techniques, we have studied maturational changes in cortical sulcal asymmetries (Blanton and others 2001; Sowell, Thompson, Rex, and others 2002), cortical gray matter asymmetries (Sowell, Thompson, Peterson, and others 2002), cortical gray matter density (Sowell, Thompson, and others 2001; Thompson, Vidal, and others 2001; Sowell, Thompson, Peterson, and others 2002; Sowell and others 2003), and brain growth (Sowell, Thompson, and others 2001). Combined, these studies have highlighted regional patterns of cortical change with age during childhood and adolescence that have not been appreciated with other image analysis techniques.

Sulcal Asymmetries. Asymmetries in sulcal patterns are of considerable interest, particularly in the peri-Sylvian cortices given the functional lateralization of language in this region (reviewed in Geschwind and
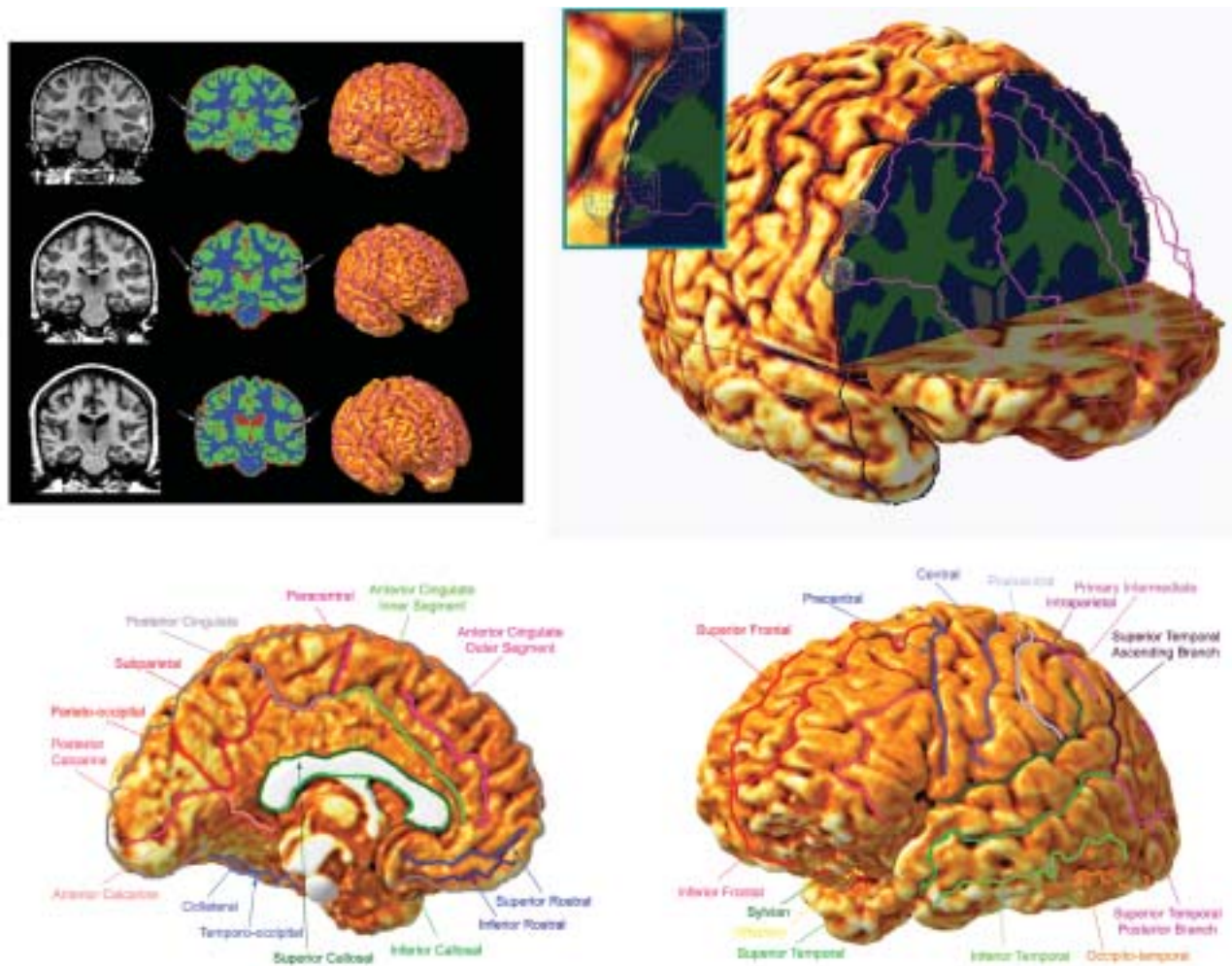
Fig. 3. *Top left*, Three representative brain image data sets with the original MRI, tissue-segmented images, and surface renderings, with sulcal contours shown in pink. *Top right*, Surface rendering of one representative subject with cutout showing tissue-segmented coronal slice and axial slice superimposed within the surface. Sulcal lines are shown where they would lie on the surface in the cutout region. Note the sample spheres over the right hemisphere inferior frontal sulcus (lower sphere) and on the middle region of the pre-central sulcus (upper sphere) that illustrate varying degrees of gray matter density. In the blown-up panel, note that the upper sphere has a higher gray matter density than does the lower sphere as it contains only blue pixels (gray matter) within the brain. The lower sphere also contains green pixels (white matter) that would lower the gray matter proportion within it. In the actual analysis, the gray matter proportion was measured within 15-mm spheres centered across every point over the cortical surface. *Bottom*, Sulcal anatomical delineations are defined according to color. These are the contours drawn on each individual's surface rendering according to a reliable, written protocol (Sowell, Thompson, Rex, and others 2002).

Galaburda 1985). Postmortem studies have shown that in adults, the Sylvian fissure is longer in the left hemisphere than the right (Galaburda and others 1978; Ide and others 1996), and in vivo vascular imaging studies have shown that the Sylvian fissure angles up more dramatically at its posterior end in the right hemisphere than the left (LeMay and Culebras 1972). Left hemisphere peri-Sylvian asymmetries greater than right hemisphere peri-Sylvian asymmetries (planum temporale length) have also been observed in postmortem studies of infants (Witelson and Pallie 1973), indicating that these asymmetry patterns may be independent of maturational change and the acquisition of language abilities

throughout infancy and childhood. Until our recent in vivo imaging studies, little was known about the emergence of cortical surface gyral and sulcal asymmetries in normal development.

Age differences in structural asymmetries at the cortical surface were mapped in groups of normally developing children (7 to 11 years), adolescents (12 to 16 years), and young adults (23 to 30 years) using the novel surface-based cortical pattern–matching image analytic methods described above. We found that asymmetries in peri-Sylvian cortices continued to develop between childhood and young adulthood (Sowell, Thompson, Rex and others 2002). Although the normal left longer than right
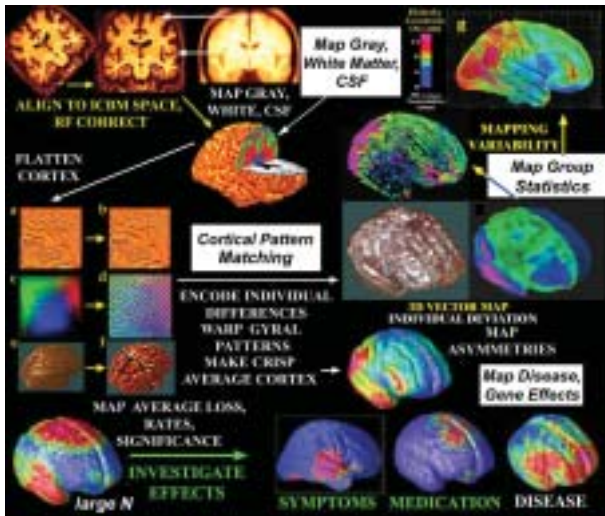
Fig. 4. Analyzing cortical data. The schematic shows a sequence of image-processing steps that can be used to map how aging affects the cortex. The steps include aligning MRI data to a standard space, tissue classification, and cortical pattern matching as well as averaging and comparing local measures of cortical gray matter volumes across subjects. To help compare cortical features from subjects whose anatomy differs, individual gyral patterns are flattened and aligned with a group average gyral pattern (*a* to *f*). Group variability (*g*) and cortical asymmetry can also be computed. Correlations can be mapped between age-related gray matter deficits and genetic risk factors. Maps may also be generated that visualize linkages between deficits and clinical symptoms, cognitive scores, and medication effects. The only steps here that are currently not automated are the tracing of sulci on the cortex. Some manual editing may also be required to assist algorithms that delete dura and scalp from images, especially if there is very little CSF in the subdural space (Thompson, Hayashi, de Zubicaray, Janke, Sowell, and others 2003).

Sylvian fissure asymmetry was present in the children, adolescents, and adults, it was much more pronounced in adulthood, on average twice the magnitude of the asymmetry observed in children. The asymmetry in the slope of the Sylvian fissure also changed with age such that the normal pattern of right more sloped than left occurred without exception in the young adults studied and significantly less frequently in the children. These findings were consistent with the earlier postmortem literature. We observed similar asymmetry patterns in an independent group of children and adolescents, and as in our other report, Sylvian fissure asymmetry was more prominent in the adolescents than in the children (Blanton and others 2001). The dynamic age-related changes in asymmetry seemed to occur as a result of robust changes in the shape and location of the right hemisphere Sylvian fissure. The slopes of the Sylvian fissure and the superior temporal sulcus were roughly parallel in children, adolescents, and adults in the left hemisphere, but in the right hemisphere, the slope of the superior temporal sulcus remained constant despite the age-related upward slope of the Sylvian fissure (see Fig. 6). This suggests an increase in the surface area of the posterior temporal lobes in the right hemisphere, result-

ing in the increased Sylvian fissure asymmetry observed with increasing age (Sowell, Thompson, Rex, and others 2002). In a small-sample longitudinal study, we observed prominent cerebral lobar growth in the lateral temporo-parietal region in children studied at various 2- to 4-year intervals between about 7 and 15 years of age (Thompson, Giedd, and others 2000), and we also observed brain growth in the inferior temporal cortex in another study (Sowell, Thompson, and others 2001). Together, these results suggest that brain growth in regions surrounding the Sylvian fissure can affect its morphology during development.

In another report, we focused on detailed three-dimensional quantitative maps of brain surface and gray matter density asymmetry patterns during normal adolescent development (Sowell, Thompson, Peterson, and others 2002). We studied two independent samples of normally developing children, adolescents, and young adults, totaling 83 subjects from two different research groups. We found that the most prominent gray matter asymmetry at the brain surface was in the posterior temporal lobes, whether looking at children, adolescents, or young adults (see Fig. 7). This finding was confirmed in two independent samples of normal control subjects scanned on different scanners by different research groups, further establishing the validity of the results. Age effects in gray matter asymmetry between the normal child and adolescent groups and between the adolescent and young adult groups were not significant, suggesting that the pattern of gray matter asymmetry is established early in development. Right greater than left gray matter asymmetry in the posterior, superior temporal sulcus has previously been reported in a large imaging study of young adults (Watkins and others 2001). White matter asymmetry in this region has also been examined by another research group, showing left greater than right white matter asymmetry in the primary auditory cortex (Penhune and others 1996), a region anterior to that observed here. Left greater than right white matter asymmetry in the posterior temporal lobes has been reported in the postmortem literature as well (Anderson and others 1999). Although we measured gray matter asymmetry, it is possible that we measured less gray matter in the left hemisphere because there was actually more white matter present with an opposite pattern in the right hemisphere. Thus, the white matter asymmetry findings from postmortem and in vivo samples may be consistent with the gray matter results reported here and by other research groups (Watkins and others 2001).

In the same group of control subjects, we assessed total brain surface asymmetry by mapping the distance from matched surface points in the left hemisphere to the same locations in the reflected right hemisphere (ignoring the large interhemispheric difference across the brain) (Sowell, Thompson, Peterson, and others 2002). Results from these analyses are shown in Figure 8. The arrows show the magnitude and direction of asymmetry at each brain surface point. Peak brain surface asymme-
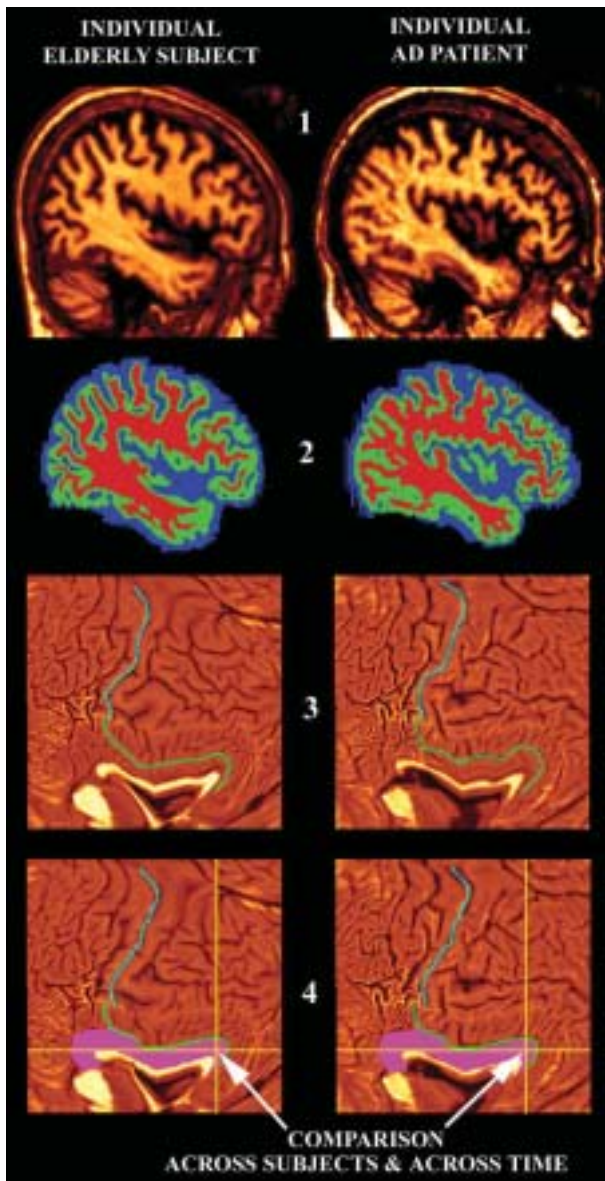
INDIVIDUAL ELDERLY SUBJECT

INDIVIDUAL AD PATIENT

1

2

3

4

COMPARISON ACROSS SUBJECTS & ACROSS TIME

Fig. 5. Comparing gray matter across subjects. Gray matter is easier to compare across subjects if adjustments are first made for the gyral patterning differences across subjects. This adjustment can be made using cortical pattern matching (Thompson, Mega, and others 2000), which is illustrated here on example brain MRI data sets from a healthy control subject (*left column*) and from a patient with Alzheimer's disease (*right column*). First, the MRI images (stage 1) have extracerebral tissues deleted from the scans, and the individual pixels are classified as gray matter, white matter, or CSF (shown here in green, red, and blue colors; stage 2). After flattening a three-dimensional geometric model of the cortex (stage 3), features such as the central sulcus (light blue curve) and cingulate sulcus (green curve) may be reidentified. An elastic warp is applied (stage 4) moving these features, and entire gyral regions (pink colors), into the same reference position in "flat space." After aligning sulcal patterns from all individual subjects, group comparisons can be made at each two-dimensional pixel (yellow cross-hairs) that effectively compare gray matter measures across corresponding cortical regions. In this illustration, the cortical measure that is compared across groups and over time is the amount of gray matter (stage 2) lying within 15 mm of each cortical point. The results of these statistical comparisons can then be plotted back onto an average three-dimensional cortical model made for the group, and significant findings can be visualized as color-coded maps. Such algorithms bring gray matter maps from different subjects into a common anatomical reference space, overcoming individual differences in gyral patterns and shape by matching locations point-by-point throughout the cortex. This enhances the precision of intersubject statistical procedures to detect localized changes in gray matter (Thompson, Hayashi, de Zubicaray, Janke, Sowell, and others 2003).

try was observed in the peri-Sylvian region where the distance between anatomically homologous surface points in the left and sulcally matched right brain surface was between 6 and 12 mm. The asymmetry was characterized by posterior displacement of the left posterior temporal and inferior parietal cortex relative to the right, similar to the results from sulcal asymmetry patterns in the same brain region (Blanton and others 2001; Sowell, Thompson, Rex, and others 2002). Vector maps showed that the direction of displacement between hemispheres in all brain regions was primarily in the anterior-posterior axis and arose primarily from the left being more posterior than the right.

Gray Matter Changes. As described above, the VBM studies have begun to shed light on the localization of tissue changes within the developing brain. We have applied cortical-matching techniques to assess maturational changes in gray matter density (Sowell, Thompson, and others 2001) that may not have been appreciated with the gross anatomical matching of the VBM studies. Thirty-five individuals between 7 and 30 years of age were assessed. Statistical maps for gray matter density differences (Fig. 9) between children and adolescents and between adolescents and adults reveal distinct patterns as expected given earlier VBM results (Sowell, Thompson, Holmes, Batth, and others 1999;
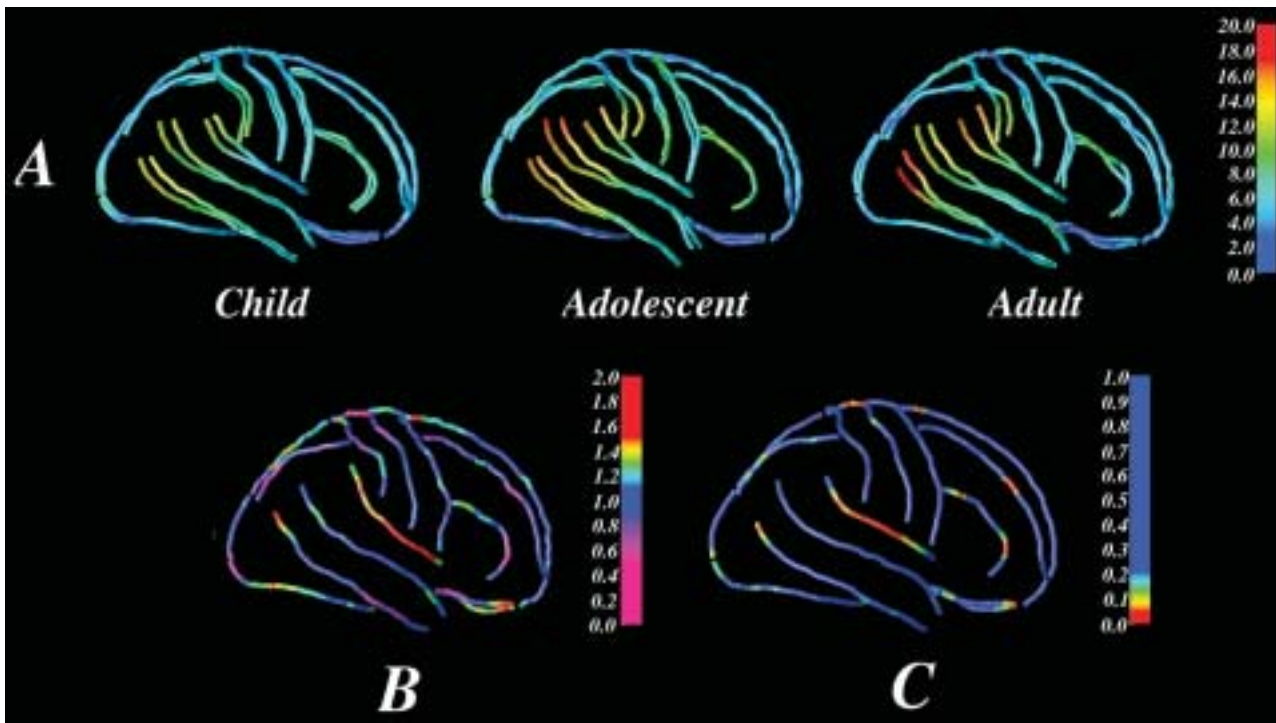
Fig. 6. *A*, Asymmetry maps for the child, adolescent, and adult groups were created by subtracting the sulcal mesh averages of one hemisphere from the mirror of the other hemisphere to create vectors representing displacement asymmetry (in millimeters) in the superior-inferior and anterior-posterior directions shown in color. These maps not only illustrate the average sulcal asymmetry in color but also show differences in sulcal shape profiles between the hemispheres because the right hemisphere is mapped onto the mirror of the left hemisphere and vice versa. Thus, the color coding is identical in the two hemispheres, but the shape of the right hemisphere sulci can be seen as distinct from the left hemisphere sulci. Note the left and right Sylvian fissures are close together (about 11 mm displacement) in the children and more splayed (about 16 mm displacement) in the young adults. *B*, Ratio map of the asymmetry at each point on each sulcus (i.e., the distance in millimeters between analogous points on sulcal curves in one brain hemisphere and a mirror image of the opposite hemisphere) in the average child to the asymmetry at each point on each sulcus in the average adult. Increases and decreases are represented in color, where red regions are indicative of increases in asymmetry with age and pink regions are representative of decreases in asymmetry with age (according to the color bar on the right). Note the prominent increase in asymmetry over the length of the Sylvian fissure. Only one hemisphere is represented, as it is a composite ratio measure of the right and left hemispheres combined (*C*). Probability map of the difference in asymmetry between the child group and the adult group represented as *P* values (for age group effect on asymmetry between children and young adults) at each point along each sulcal curve according to the color bar on the right. The age group effect on asymmetry is significant for the Sylvian fissure ($P = 0.041$) as determined with permutation tests (Sowell, Thompson, Rex, and others 2002).
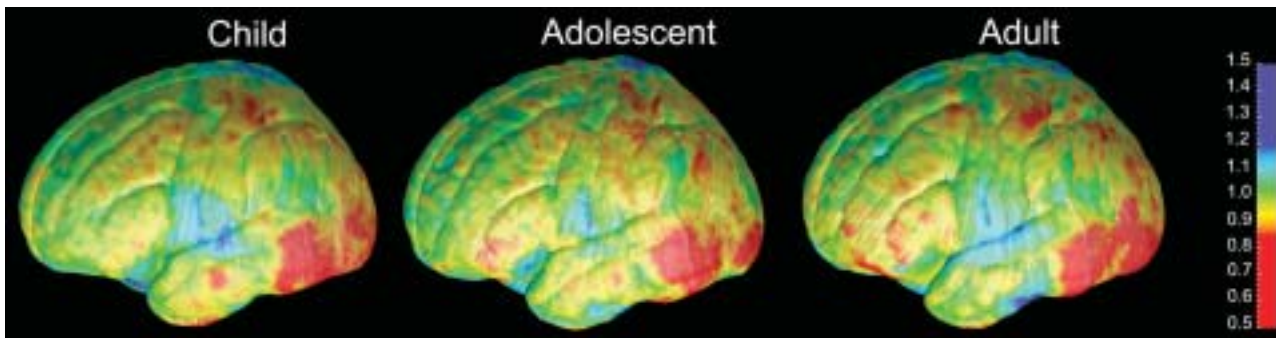

Fig. 7. Shown here are ratio maps for groups of 25 children, 15 adolescents, and 16 young adults quantifying the amount of gray matter within a 15-mm sphere at each brain surface point in the left hemisphere as ratio to that of the analogous points in the right hemisphere. According to the color bar, 1 (color coded in green shades) represents complete symmetry. Cooler colors (greater than 1) represent regions where there is more gray matter in the left hemisphere than in the right, and warmer colors (less than 1) represent regions where there is more gray matter in the right hemisphere than in the left (Sowell, Thompson, Peterson, and others 2002).
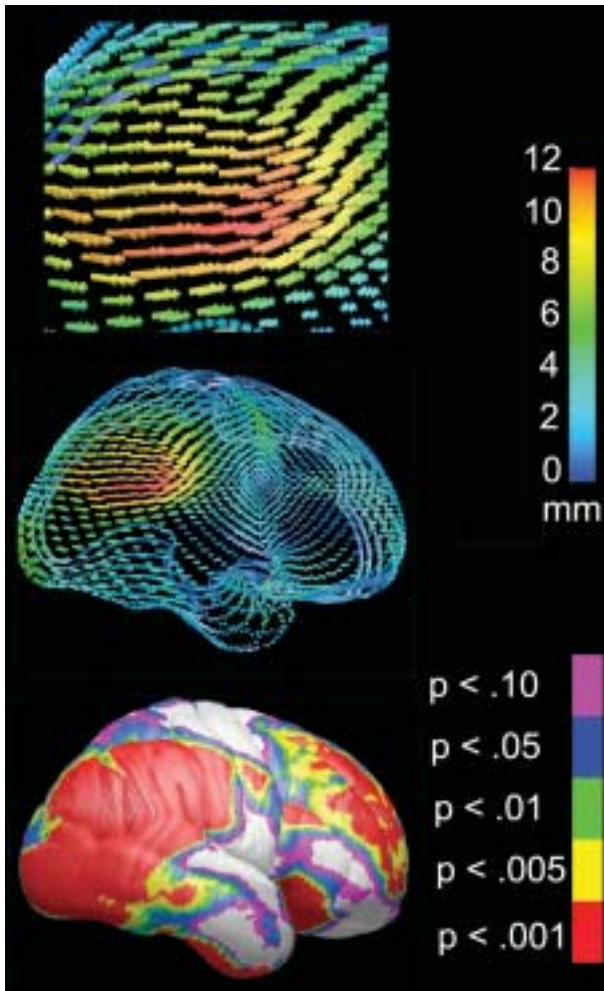
Fig. 8. The arrows in these maps show the three-dimensional direction and distance of displacement between analogous surface points in the left and right hemispheres for a group of 62 normal controls between 7 and 30 years old. The base of each arrow represents the left hemisphere surface point location, and the tip of the arrow represents the analogous surface point location in the right hemisphere (a flipped and reflected version). Group differences (in millimeters) are mapped in color according to the color bar on the right. Note maximal asymmetry, up to 12-mm difference between analogous surface points is found in the peri-Sylvian region, shown enlarged to enhance detail in the top row. Displacement between left and right hemispheres is primarily in the anterior-posterior axis in most regions, more prominent in the peri-Sylvian region. Statistical maps are shown in the bottom row documenting the significance of displacement between analogous surface points in the left and right hemispheres according to the color bar (note white regions are $P > 0.10$). Note that we have assessed the significance of displacement in only the anterior-posterior direction because that is the primary direction of displacement in the peri-Sylvian region. The probabilities shown are for negative correlation coefficients (left more posterior than right surface point location), as few positive correlation coefficients reached statistical significance and they were all on the inferior surface of the brain not shown here (Sowell, Thompson, Peterson, and others 2002).

Sowell, Thompson, Holmes, Jernigan, and others 1999). Between childhood and adolescence, local gray matter density loss was distributed primarily over the dorsal frontal and parietal lobes. Similar effects of gray matter density reduction were observed in a small, independent longitudinal sample of normal adolescents who were studied as controls for patients with schizophrenia (Thompson, Vidal, and others 2001). Between adolescence and adulthood, a dramatic increase in local gray matter density loss was observed in the frontal lobes, parietal gray matter loss was reduced relative to the earlier years, and a relatively small, circumscribed region of local gray matter density increase was observed in the left peri-Sylvian region. Unlike in our previous reports, with sulcal pattern matching, we were able to statistically map the significance of differences between child-to-adolescent and adolescent-to-adult contrasts, finally confirming that there are regions of accelerated gray matter loss in the postadolescent age range, mostly in the dorsal frontal cortices (see Fig. 9). These findings suggest that changes in gray matter density between childhood and young adulthood may not be linear in nature.

Brain Growth. In this same group of 35 subjects, we also assessed localized brain growth using our distance from center (DFC) measure. It is a measure of radial expansion measured from the center of each subject's brain roughly at the midline decussation of the anterior commissure (i.e., $x = 0$, $y = 0$, $z = 0$) to each of the 65,536 matched brain surface points. Differences in the length of the DFC line at each brain surface point between groups (i.e., children and adolescents) suggest local growth in that location, and statistical analyses at each point can be conducted, much like with gray matter density. We found statistically significant spatial and temporal patterns of brain growth and surface contraction between childhood, adolescence, and young adulthood. Because the brain surfaces were scaled to remove global size differences for these analyses, local brain growth and contraction observed in these results must be considered relative to global differences in brain size between groups. Notably, the relative maps reveal little local growth (increased DFC) occurring between childhood and adolescence (Fig. 10) once overall brain size differences are controlled. When comparing the adolescents to the adults, there was some regional specificity with prominent local growth or increased DFC occurring in the dorsal aspects of the frontal lobes bilaterally in the same general region where we observed accelerated gray matter density reduction described above. Lateral growth also appeared in the inferior, lateral temporo-occipital junction bilaterally where the brain surface was also significantly farther from the center of the brain in the adults than in the adolescents. Finally, some growth was also observed in the orbital frontal cortex, more prominent in the left hemisphere. The difference between
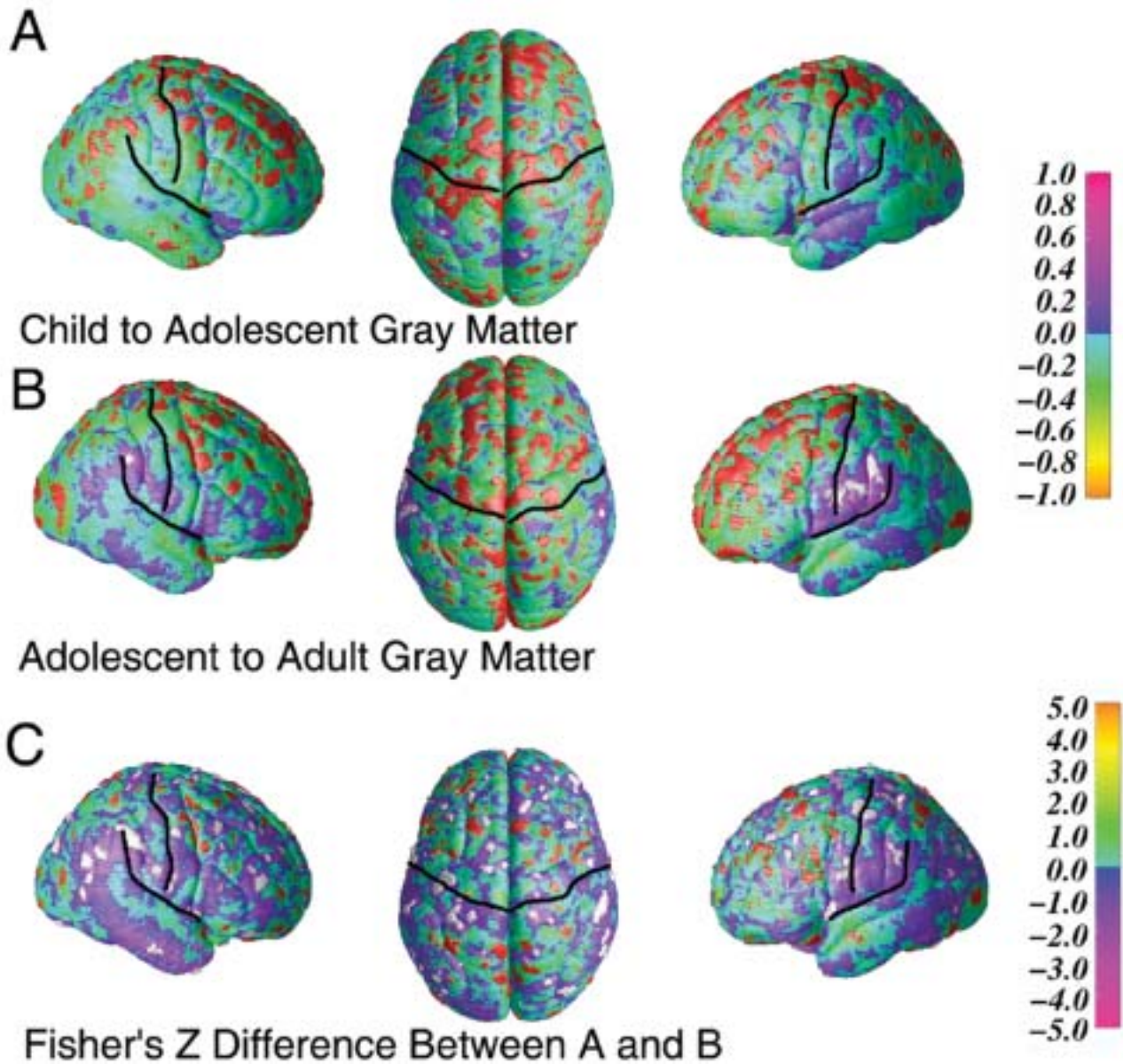
Fig. 9. Gray matter density age effect statistical maps (left, right, and top views) showing gray matter density changes between childhood and adolescence (*top*) and between adolescence and adulthood (*middle*). Anatomically, the central sulcus (CS), Sylvian fissure (SF), and interhemispheric fissure (IF) are highlighted. In both images, shades of green to yellow represent negative Pearson's correlation coefficients (gray matter loss with increasing age) and shades of blue, purple, and pink represent positive Pearson's correlation coefficients (gray matter gain with age) according to the color bar on the right (range of Pearson's correlation coefficients from −1 to +1). Regions shown in red correspond to correlation coefficients that have significant negative age effects at a threshold of $P = 0.05$ (gray matter loss), and regions shown in white correspond to significant positive age effects at a threshold of $P = 0.05$ (gray matter density gain). The images on the bottom display a statistical map of the Fisher's Z transformation of the difference between Pearson's correlation coefficients for the child-to-adolescent and the adolescent-to-adult contrasts (see color bar on far right representing Z scores from −5 to +5). Shades of green to yellow represent regions where the age effects are more significant in the adolescent-to-adult contrast (*middle*) than in the child-to-adolescent contrast (*left*). Highlighted in red are the regions where the difference between Pearson's correlation coefficients is statistically significant ($P = 0.05$). Shades of blue, purple, and pink represent regions where the age effects are more significant in the child-to-adolescent contrast than in the adolescent-to-adult contrast. Highlighted in white are regions where these effects are significant at a threshold of $P = 0.05$ (Sowell, Thompson, and others 2001).

correlation coefficients for the child-to-adolescent and adolescent-to-adult comparisons shown in Figure 10 confirmed the accelerated local growth in dorsal frontal regions in the older age range and accelerated local growth in the posterior temporo-occipital junction as well.

Brain image data sets were also assessed without scaling to adjust for brain size differences. The nonscaled
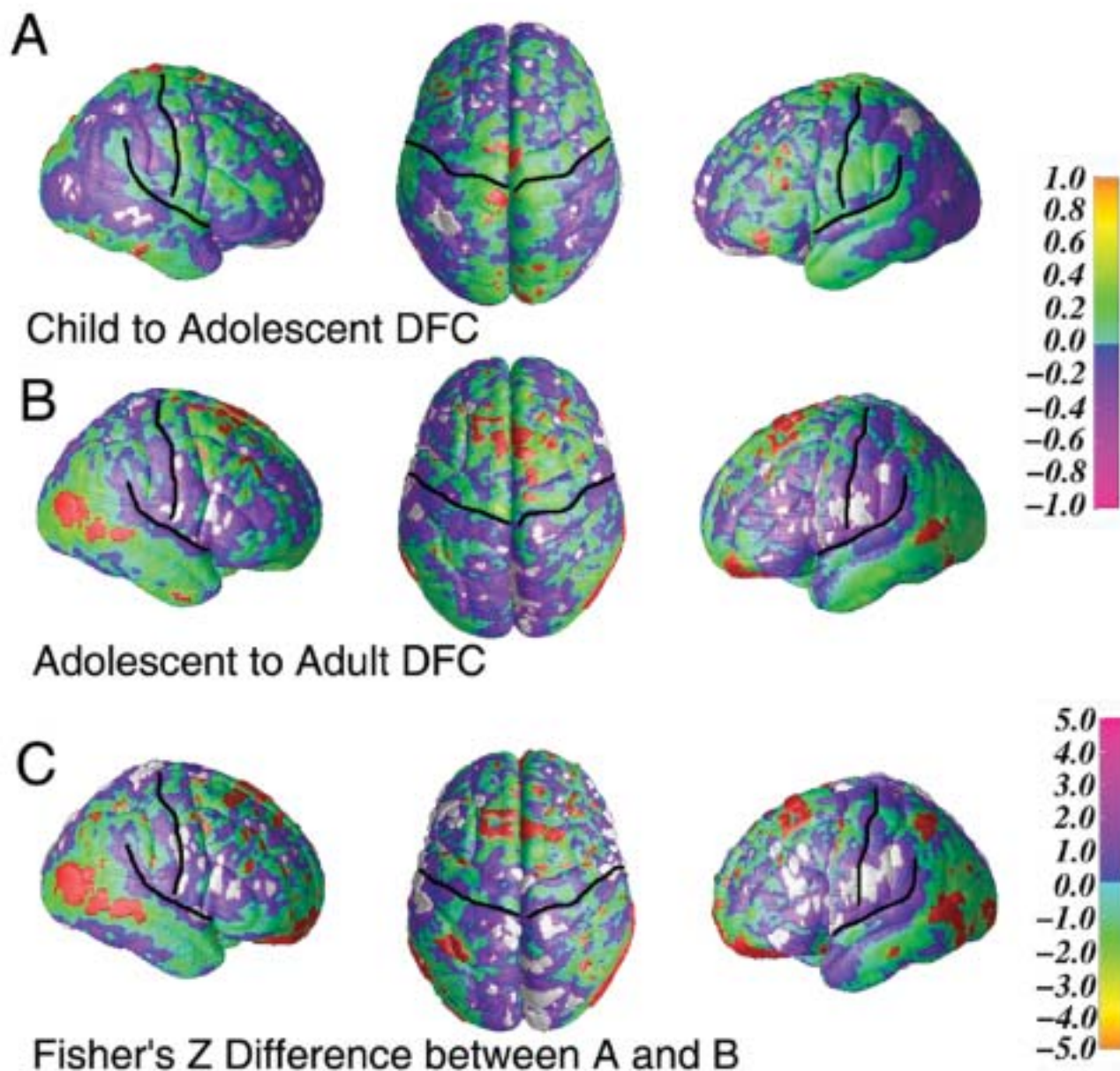
Fig. 10. Distance from center (DFC) age effect statistical maps (left, right, and top views) showing changes in DFC between childhood and adolescence (*top*) and between adolescence and adulthood (*middle*). Anatomically, the central sulcus (CS), Sylvian fissure (SF), and interhemispheric fissure (IF) are highlighted. In both images, shades of green to yellow represent positive Pearson's correlation coefficients (increased DFC or brain growth) and shades of blue, purple, and pink represent negative Pearson's correlation coefficients (decreased DFC or shrinkage) according to the color bar on the right (range of Pearson's correlation coefficients from –1 to +1). Regions shown in red correspond to correlation coefficients that have significant positive age effects at a threshold of $P = 0.05$ (brain growth), and regions shown in white correspond to significant negative age effects at a threshold of $P = 0.05$ (brain shrinkage). The images on the bottom display a statistical map of the Fisher's Z transformation of the difference between Pearson's correlation coefficients for the child-to-adolescent and the adolescent-to-adult contrasts (see color bar on far right representing Z scores from –5 to +5). Shades of green to yellow represent regions where the age effects are more significant in the adolescent-to-adult contrast (*middle*) than in the child-to-adolescent contrast (*left*). Highlighted in red are the regions where the difference between Pearson's correlation coefficients is statistically significant ($P = 0.05$). Shades of blue, purple, and pink represent regions where the age effects are more significant in the child-to-adolescent contrast than the adolescent-to-adult contrast. Highlighted in white are regions where these effects are significant at a threshold of $P = 0.05$. Note that the sign of the differences between contrasts is opposite to that in the difference map for the gray matter density contrasts because of the inverse relationship between gray matter density (negative effects) and late brain growth (positive effects) (Sowell, Thompson, and others 2001).

maps showed that continued brain growth occurred between adolescence and adulthood in the most extreme dorsal aspects of the posterior frontal lobes bilaterally and in the posterior inferior temporal lobes bilaterally whether or not brain size differences were controlled. As shown in Figure 11, between adolescence and adulthood,
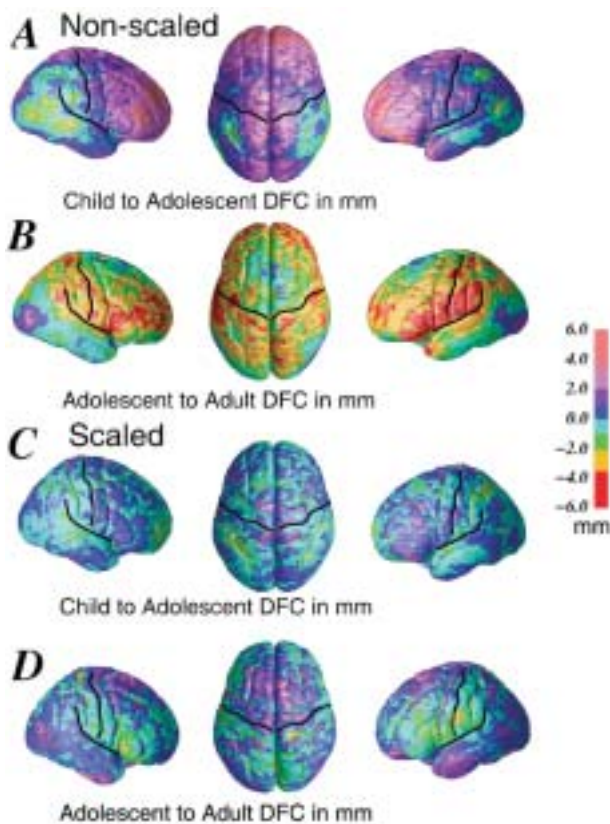
Fig. 11. Differences between groups in distance from center (DFC) shown in millimeters in color (according to the color bar) between childhood and adolescence in both nonscaled (*A*) and scaled image data sets (*C*). Differences between adolescents and adults are also shown in nonscaled (*B*) and scaled images (*D*). Anatomically, the central sulcus (CS) and Sylvian fissure (SF) are highlighted. The maps in scaled image space allow an assessment of the magnitude (in millimeters) of differences in DFC shown as statistical maps in Figure 10. The same color scale applies to both nonscaled and scaled images, and regions of brain growth between the younger and older age groups tested are shown in dark blue, purple, and pink, and regions of shrinkage between the younger and older groups tested are shown in red, yellow, green, and light blue. Note that whether or not brain size correction is made with scaling, dorsal frontal lobes and posterior temporal lobes show evidence for continued growth after adolescence. Other less robust regions of brain growth or shrinkage are "scaled" out when brain size correction is used to control individual differences (Sowell, Thompson, and others 2001).

large, diffuse regions of shrinkage or decreased DFC were observed in frontal and parietal regions surrounding the frontal and temporal growth areas. This was in contrast to the large regions of growth in frontal cortices between childhood and adolescence, with shrinkage occurring only in parietal and inferior temporal cortices bilaterally. These regions of growth and shrinkage were not as prominent in the analyses of scaled image data sets when overall differences in brain size were corrected. The analyses of nonscaled images do suggest that much of the progressive maturational change that leads to the subtle increase in total brain size occurs during the years between childhood and adolescence. Only relative-

ly subtle growth occurs after adolescence in dorsal frontal and posterior temporal cortices.

Relationships between Brain Growth and Gray Matter Density Reduction. Notably, when comparing the adolescents to the adults, significant gray matter density loss in the frontal lobes was seen almost exclusively in locations where positive age effects for DFC were observed, with very little gray matter loss observed in frontal regions that were not growing in this age range. In the composite map shown in Figure 12, the regions of significant gray matter loss overlapped nearly perfectly onto the regions of frontal lobe brain growth in the correlation map for DFC. It is interesting to note the correspondence in the distributions of these two features of brain development (brain growth and gray matter density reduction) despite their irregular shapes and patterns over the brain surface. Similar effects were observed in the child-to-adolescent comparison composite map where significant gray matter loss tended to be seen primarily in regions where growth was observed, although these effects were in different regions than those in the adolescent-to-adult age range. The strong correspondence in the age effects for gray matter density reduction and increased brain growth in the frontal cortex may provide new insight for making inferences about the cellular processes contributing to postadolescent brain maturation.

Aging

Fewer studies of aging than maturation have been conducted using the cortical pattern–matching techniques described in this review. We have conducted one comprehensive study of gray matter changes across the human life span (7 to 87 years) in a group of 176 normal individuals (Sowell and others 2003). Groups of elderly normal subjects have been studied as controls for patients with Alzheimer's disease, shedding further light on aging processes in cortical asymmetries (Thompson and others 1998) and gray matter density changes (Thompson, Hayashi, de Zubicaray, Janke, Rose and others 2003).

Sulcal Asymmetry Patterns. Sulcal pattern asymmetry measures in 10 normal elderly subjects (Thompson and others 1998) were similar to those observed in normal children, adolescents, and young adults (Sowell, Thompson, Rex, and others 2002). Relatively small asymmetries were observed in parieto-occipital, anterior and posterior calcarine, and cingulate sulci (between 3- and 4-mm difference between left and right hemispheres). Robust asymmetries were observed in the Sylvian fissure, with an upward slope of the right hemisphere relative to the left and elongation of the left hemisphere relative to the right. The distance between matching anatomical points in the left and right Sylvian fissures was maximal at 14 mm. Brain surface asymmetry was studied in a larger group of 20 elderly control subjects, showing a similar pattern of poste-
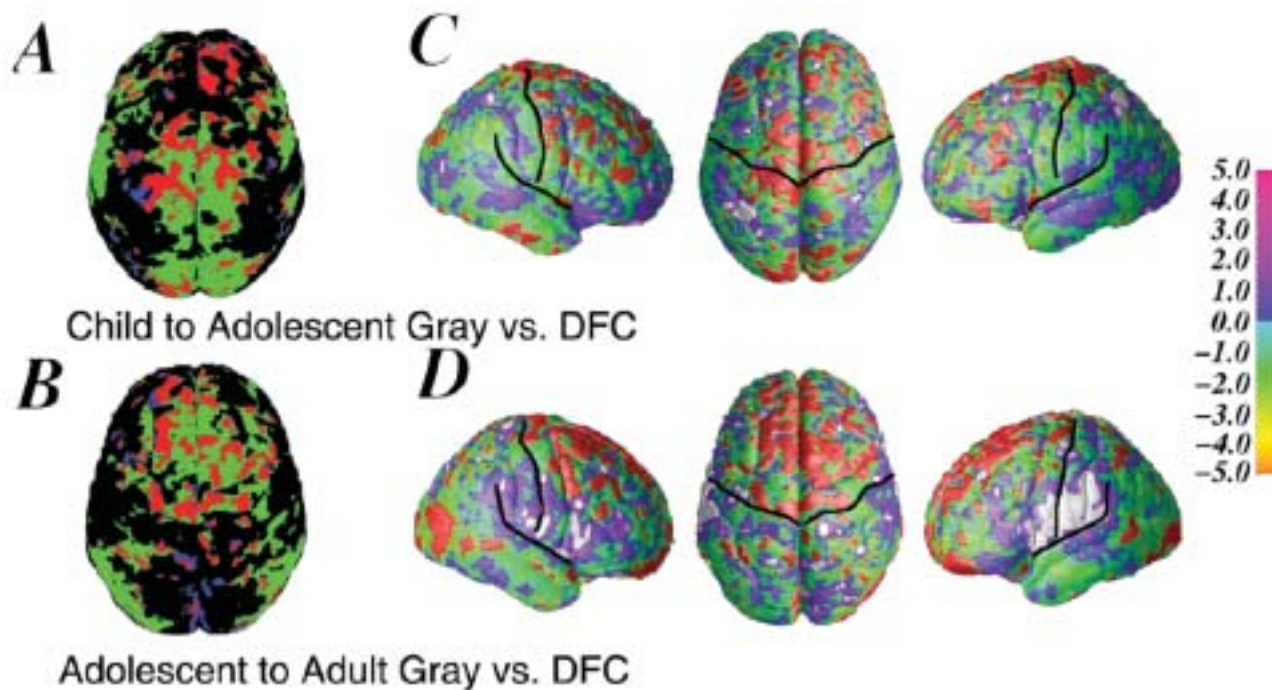
Fig. 12. Composite statistical maps (*top*) showing the correspondence in age effects for changes in distance from center (DFC) and changes in gray matter in the child-to-adolescent contrast (*A*). Shown in green is the Pearson's *R* map of all positive correlation coefficients for DFC (shown also in Fig. 10), and in blue is the probability map of all regions of significant gray matter loss (surface point significance threshold $P = 0.05$, as shown in Fig. 9). In red are regions of overlap in the gray and DFC statistical maps. A similar composite map for the adolescent-to-adult age effects is also shown (*B*). Note the highly spatially consistent relationship between brain growth and reduction in gray matter density. The shapes of the regions of greatest age-related change for the two maps (gray matter and DFC) are nearly identical in many frontal regions in the adolescent-to-adult contrast. Very few regions of gray matter density reduction fall outside regions of increases in DFC. Shown in images in the lower part of this figure (*left*, *right*, and *top* views) are the difference between Pearson's correlation coefficients for the age effects for gray matter density and the age effects for DFC between childhood and adolescence (*C*) and between adolescence and adulthood (*D*). These maps are similar to the difference between correlation coefficients for age effects of gray matter and DFC shown in Figures 9 and 10 but instead highlight the correlation between regions of greatest change in the two separate features of brain maturation measured here (DFC and gray matter density). The color bar represents corresponding *Z* scores ranging from −5 to +5 for the difference between correlation coefficients for DFC and gray matter. Highlighted in red are regions of significant negative correlations between DFC and gray matter density ($P = 0.05$), showing that the relationship between regions of greatest gray matter density reduction are statistically the same as the regions with the greatest brain growth, particularly in the adolescent-to-adulthood years. Highlighted in white are the regions where the difference between correlation coefficients for the gray matter and DFC maps is positive, indicating that the change with age is in the same direction for both variables (i.e., increased DFC change goes with increased gray matter density change) (Sowell, Thompson, and others 2001).

rior displacement of the left peri-Sylvian region relative to the right (Thompson, Mega, Vidal, and others 2001). In another study, 28 normal adults (mean age = 30.5 years) were assessed as controls for patients with schizophrenia, and Sylvian fissure asymmetry was also maximal at approximately 14 mm in the most posterior extent of this structure (Narr and others 2001). Thus, in all populations studied to date—children (Blanton and others 2001; Sowell, Thompson, Rex, and others 2002), adolescents (Sowell, Thompson, Rex, and others 2002), young adults (Sowell, Thompson, Rex, and others 2002), adults (Narr and others 2001), and elderly (Thompson and others 1998)—sulcal asymmetries are most prominent in the posterior Sylvian fissure with upward shifts of the right relative to the left and elongation of the left relative to the right.

Gray Matter Density. In a recent report (Sowell and others 2003), we used cortical-matching algorithms to create three-dimensional, nonlinear statistical, and peak age maps of gray matter density change on the lateral and interhemispheric brain surfaces across nine decades (7 to 87 years) in 176 normal individuals. Significant, nonlinear age effects were observed over large areas of the most dorsal aspects of the frontal and parietal regions on both the lateral and interhemispheric surfaces and in the orbit frontal cortex (Fig. 13). Scatter plots of these effects revealed a dramatic decline in gray matter density between the ages of 7 and 60 years, with little or no decline thereafter. A sample scatter plot of the quadratic effect of age on gray matter density at one brain surface point on the superior frontal sulcus is also shown in Figure 13 and is similar to others in the dorsal frontal and parietal regions (see Fig. 14). In the superior frontal sulcus, there was a loss of gray matter density of approximately 32% between the ages of 7 and 60 years, declining to only 5% loss between the ages of 40 and 87 years. Notably, the most lateral aspects of the brain in the pos-
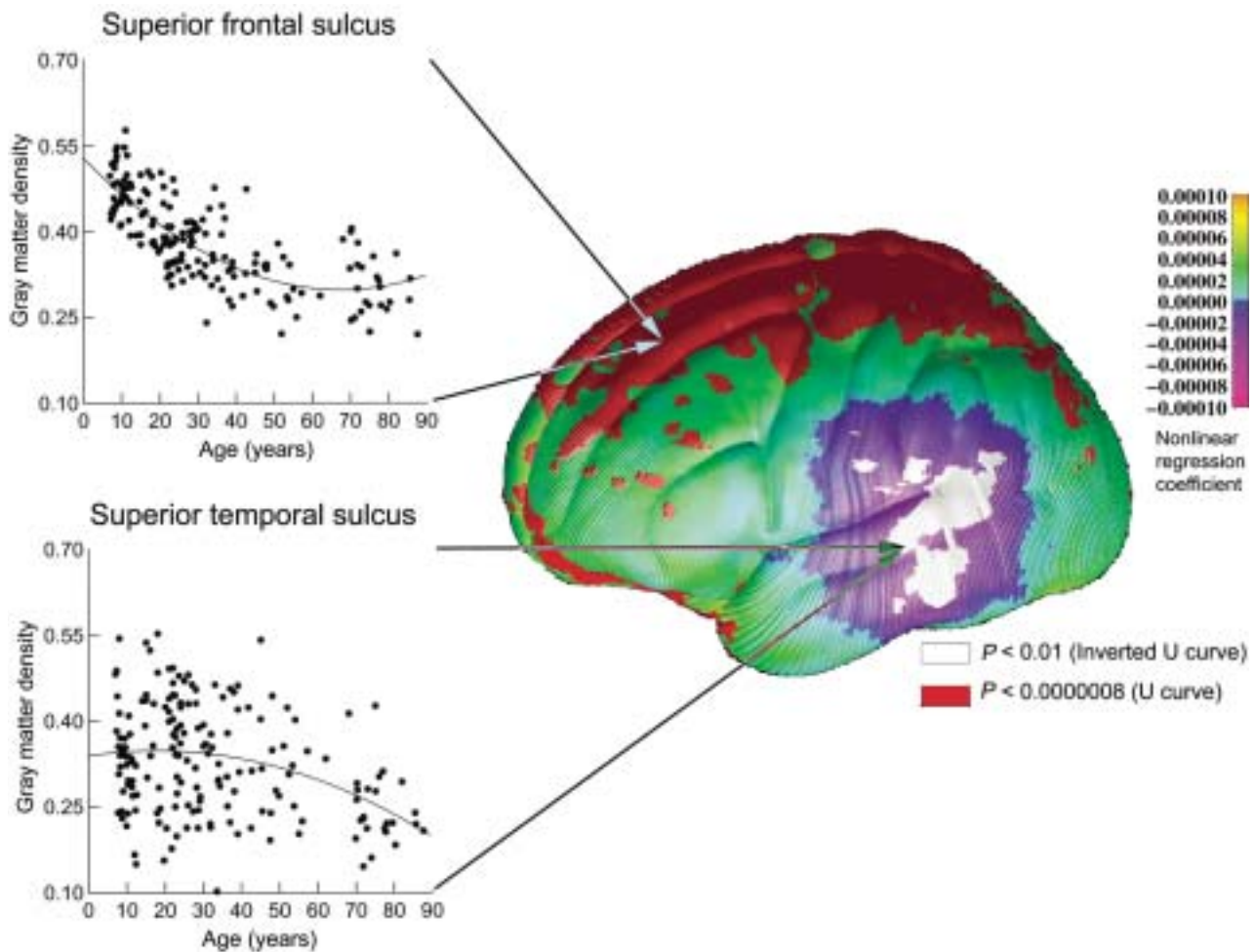
Fig. 13. This map (left frontal view) shows age effects on gray matter density on the lateral surface of the brain between childhood and old age. Shades of green to yellow represent positive partial regression coefficients for the quadratic term (U-shaped curves with respect to age), and shades of blue, purple, and pink represent negative partial regression coefficients (inverted U-shaped curves). Regions shown in red correspond to regression coefficients that have significant positive nonlinear age effects at a threshold of P = 0.0000008, and regions shown in white correspond to significant negative nonlinear age effects at a threshold of P = 0.01. The pattern of nonlinear age effects was similar in the left and right hemispheres (not shown) except that none of the negative nonlinear age effects in the right posterior temporal lobe reached a threshold of P = 0.01. Scatter plots of age effects with the best-fitting quadratic regression line are shown for sample surface points in the superior frontal sulcus (*top*) and the superior temporal sulcus (*bottom*), representative of the positive (U-shaped) and negative (inverted U-shaped) nonlinear age effects. Gray matter proportion within the 15-mm sphere surrounding the sample surface point (matched across subjects) is shown on the *y*-axis (Sowell and others 2003).

terior temporal and inferior parietal lobes bilaterally show a different pattern, one in which the nonlinear age effects were inverted relative to the age effects seen in more dorsal cortices. A subtle increase in gray matter density was observed until age 30, which remained stable until a precipitous decline was seen in later decades (Figs. 13 and 14). In contrast to the percentage changes reported above for the superior frontal sulcus, only a 12% decline in gray matter density was observed in the superior temporal sulcus between the ages of 7 and 60 years, increasing to a 24% decline between the ages of 40 and 87 years. Intriguingly, the rapid decline in gray matter density in these lateral regions occurred when the age effects in the dorsal surfaces leveled off. Interindividual variability in gray matter density was accentuated in these regions, contributing to less signif-

icant age effects here than on the more dorsal surface of the brain.

The age at base gray matter loss (lowest point in the quadratic curve) or peak gray matter gain (in the posterior temporal lobes) was estimated for each brain surface point and mapped onto the average brain surface rendering (Fig. 15). Base gray matter density levels in the most dorsal aspects of the parietal lobes seem to hit their nadir earlier (at 40–50 years) than do the frontal lobes (at 50–60 years). The peak age maps show an intriguing pattern of age effects in which the association cortices of the frontal and parietal lobes show the most robust gray matter density loss early in life, and primary auditory (lateral surface) and visual cortices show a much shallower decline over the life span (see regions color coded in black in Fig. 15).

Fig. 14. Shown is a surface rendering of a human brain (left hemisphere; left is anterior, right is posterior) with scatter plots for gray matter density at various points over the brain surface. The graphs are laid over the brain approximately where the measurements were taken. The axes for every graph are identical, and they are identical to the axes on graphs shown in Figure 13 (Sowell and others 2003).

The regionally and temporally variable patterns of aging on gray matter density probably reflect differences in the underlying cellular architecture in those regions and likely contribute to the well-documented variability in cognitive functions associated with aging. We have shown correlations between IQ and localized differences in gray matter density between normal adult twins (Thompson, Cannon, and others 2001). Although we cannot directly measure myelin deposition, somal size, or synaptic density using MRI, postmortem studies described above indicate that these cellular changes occur simultaneously throughout maturation and aging.

Summary of Cortical Pattern–Matching Analyses

The cortical pattern–matching studies of maturation and aging have shown various regional patterns of changing peri-Sylvian asymmetries, gray matter changes, and brain growth, depending on the age range studied. The general pattern of asymmetry in the posterior temporal lobe is remarkably similar across all subject samples and age ranges studied, with longer left than right and more sloped right than left Sylvian fissures (Thompson and others 1998; Blanton and others 2001; Narr and others 2001; Sowell, Thompson, Rex, and others 2002). However, there is an increase in the magnitude of this asymmetry between childhood and adulthood, as shown in one of the studies (Sowell, Thompson, Rex, and others 2002), probably related to regional growth in cortical structures surrounding the Sylvian fissure. Age effects in this sulcal pattern asymmetry beyond young adulthood have not been studied, despite the fact that numerous normal populations across the age span from child-hood to old age have been assessed with the same image analysis methods. This is largely because comparability of data collected on different magnets with different image acquisition protocols and by different research groups has not been assessed under these circumstances, rendering it difficult to make direct comparisons. Experience-dependent plasticity and asymmetries in behavioral function may be responsible for differential maturational patterns between the two hemispheres. For a recent, thorough review of the functional significance of brain asymmetries, see Toga and Thompson (2003).

Age-related changes in cortical surface gray matter density patterns have been consistent across populations and vary depending on the age group studied. Gray matter density reduction has been observed during adolescence both cross-sectionally (Sowell, Thompson, and others 2001; Sowell and others 2003) and longitudinally (Thompson, Vidal, and others 2001). These findings are generally consistent with the volumetric imaging literature (Giedd and others 1999; Sowell, Trauner, and others 2002) and VBM studies (Sowell, Thompson, Holmes, Batth, and others 1999; Sowell, Thompson, Holmes, Jernigan, and others 1999). Regional patterns suggest that gray matter density reduction in parietal cortices begins earlier in childhood, followed by the frontal lobes when more prominent gray matter loss occurs between adolescence and adulthood (Sowell, Thompson, Holmes, Batth, and others 1999; Sowell, Thompson, Holmes, Jernigan, and others 1999; Sowell, Thompson, and others 2001; Sowell and others 2003). In our previous report, we speculated that cognitive functions subserved by parietal association cortices (i.e., spatial relations) may develop earlier than the executive functions associated with the frontal lobes (Sowell, Thompson, Holmes, Jernigan, and others 1999). When assessed across the age span between 7 and 87 years, gray matter density decline is prominent across most dorsal cortical regions, but the gray matter loss is nonlinear in nature. Peak loss occurs in most dorsal brain regions between the ages of 50 and 70, after which there is a much more gradual decline. Interestingly, gray matter density increases also occur and are specific to primary language areas in the posterior peri-Sylvian region (i.e., Wernicke's area). These changes have been observed in two independent samples thus far, and studies across the human life span suggest that gray matter increases are occurring until approximately 30 years of age, followed by a more gradual decline than that observed in other cortical regions (Sowell, Thompson, and others 2001; Sowell and others 2003).

What is different about posterior peri-Sylvian regions that the pattern of maturation and aging appears so disparate from most other cortical regions? In our report of these findings, we speculated that specific language functions such as language comprehension skills are less vulnerable to aging, whereas more anterior language functions such as language production and word retrieval deteriorate as a function of normal aging (Sowell and others 2003). Perhaps the protracted pattern
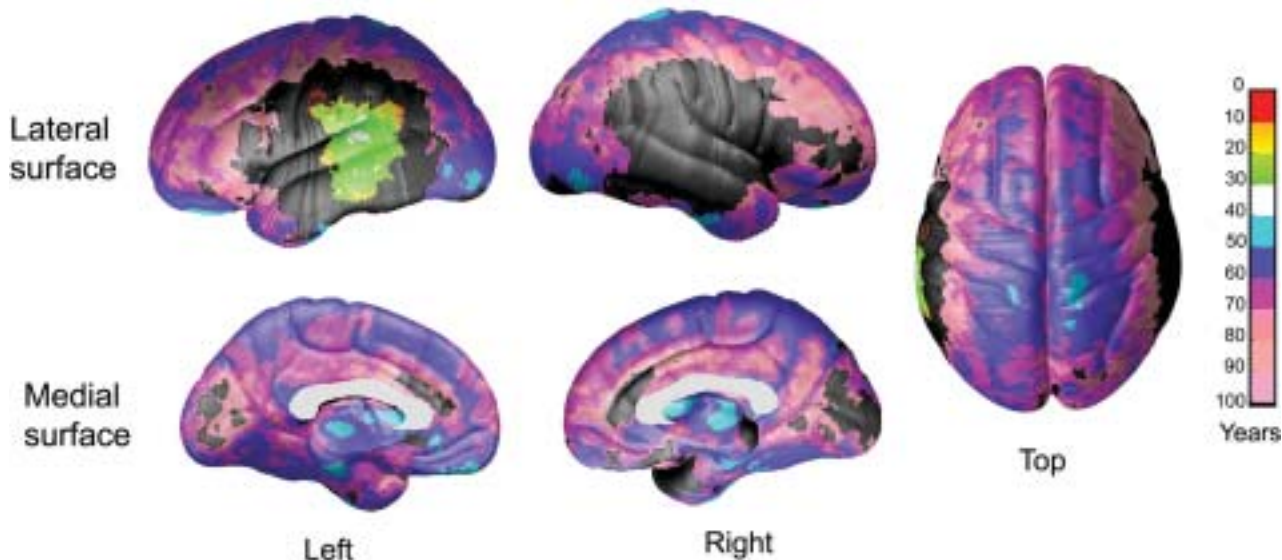
Fig. 15. Peak (or base) age maps for the nonlinear effects of age on gray matter. Shown in color, according to the color bar on the right, is the mean age at which peak or base gray matter density is reached for each point on the lateral (*top*), interhemispheric (*bottom*), and top (*right*) surface of the brain. Shown in black are regions where the partial correlation coefficient for the nonlinear age effect did not reach significance at a level of *P* = 0.05. Age effects in these regions tended to be linear, rather than quadratic (Sowell and others 2003).

of maturation and aging in these regions is related to the pattern of vulnerable and relatively invulnerable language capacities.

Finally, regional patterns of brain growth and shrinkage have suggested that the most dorsal regions of the frontal lobes continue to grow between adolescence and adulthood (Sowell, Thompson, and others 2001). Brain growth in these regions spatially and temporally coincide with regional patterns of gray matter density reduction between childhood and young adulthood. Regressive (i.e., synaptic pruning) and progressive (i.e., myelination) cellular events are known to occur concurrently in the brain during childhood, adolescence, and young adulthood, both of which could result in the appearance of gray matter density reduction or cortical thinning on MRI. A reduction in the number of synapses in the cortex could result in our observations of reduced gray matter density. On its own, this process would seem to result in a net brain volume loss (along with an increase in CSF). Notably, however, we found local brain growth in the same regions where gray matter density reduction was occurring. An increase in the amount of myelin could also result in a reduction in the amount of brain tissue that has a gray matter appearance on MRI, given that nonmyelinated peripheral axonal and dendritic fibers do not have typical white matter signal values on T1-weighted MRI (Barkovich and others 1988). Increased myelination would seem to necessarily result in a net brain volume increase, given that myelin consists of space-occupying glial cells (Friede 1989). This would be consistent with our data showing late growth in frontal cortex concomitant with the cortical gray matter density reduction.

Integration of Aging and Development with *In Vivo* and Postmortem Studies

Integrating the results from maturational and aging studies is complicated. One of the ultimate goals is to determine when maturation stops and when the more degenerative changes with aging begin. From the studies encompassing an age range between childhood and old age, it is clear that assessment of gray matter density alone cannot begin to disentangle this interesting question. Clearly, the prominent gray matter density loss that occurs between the ages of 7 and 20 has a different etiology from the continued gray matter loss that occurs between 40 and 60 years of age. We know from postmortem studies that myelination (at least in the mesial temporal lobe) peaks at approximately 50 years of age, and myelination is much more prominent between birth and approximately 20 years of age than it is from 20 to 50 years (Benes and others 1994). Brain weight is maximal by approximately 20 years of age and does not begin to decline until approximately 55 years of age (Dekaban 1978). Synaptic density loss is prominent during adolescence in a regionally variable pattern, but it continues into old age as well (Huttenlocher and Dabholkar 1997). In vivo volumetric studies show relatively consistent gray matter loss in many cortical regions beginning in late childhood (Jernigan, Trauner, and others 1991; Giedd and others 1999; Sowell, Trauner, and others 2002) and continuing apparently linearly through old age (Jernigan, Archibald and others 1991; Pfefferbaum and others 1994; Blatter and others 1995; Courchesne and others 2000; Bartzokis and others 2001; Ge and others 2002; Bartzokis and others 2003).

White matter volume, on the other hand, increases up until approximately the mid-40s (Bartzokis and others 2001; Sowell and others 2003), which coincides with the peak myelination observed at approximately age 50 (Benes and others 1994). It seems reasonable to speculate then that the gray matter loss observed during childhood and young adulthood results from a combination of synaptic pruning and increased myelination (and perhaps other cellular changes as well that result in local brain size increases concomitant with gray matter reduction) (Sowell, Thompson, and others 2001), whereas the gray matter loss that occurs later in adulthood may be more due to a combination of continued late myelination and perhaps decreased somal size (Terry and others 1987). The leveling of gray matter loss seen in late adulthood in cortical pattern–matching studies (Sowell and others 2003) may begin at a time when only degenerative changes (i.e., decreased somal size/atrophy) are occurring in the absence of continued myelination and synaptic pruning. Unfortunately, these changes would be impossible to discriminate with the conventional image acquisition protocols used in most of the structural brain-imaging studies reviewed here. A study combining postmortem and in vivo analyses of individuals across the age span could be used to determine when gray matter loss observed in vivo coincides with gray matter thinning associated with maturational versus atrophic processes. Long-range longitudinal studies along with cognitive assessments would also be ideal for disentangling maturational from degenerative changes observed in the in vivo studies.

Findings of localized gray matter density increases up to approximately age 30 in posterior language cortices are relatively new, although they have been replicated in two independent samples (Sowell, Thompson, and others 2001; Sowell and others 2003). It is somewhat more difficult to speculate on what cellular changes could be causing gray matter growth, given the postmortem studies that have been more helpful in explaining gray matter loss observed in most other cortical regions. It has been speculated that increases in gray matter volume could be related to a "second wave of over production of synapses" (Giedd and others 1999), but there does not appear to be much support for this hypothesis in the human or animal literature. It is now generally well accepted that neurogenesis does occur in the adult mammalian brain (Gould and Gross 2002). Adult-generated cells with neuronal characteristics have been found in the temporal neocortex in the monkey. It has been shown that enriched environments enhance the survival of newly generated cells (reviewed in Gould and Gross 2002). The only lateral cortical region in the brain to show prominent gray matter increases into adulthood are primary language cortices. Perhaps neuronal proliferation in humans could occur only in brain regions subserving a prominent primary cognitive function, such as language, involved in so many aspects of human cognition.

Conclusions and Future Directions

We have reviewed a variety of literatures that assess the effects of aging on the morphology of the human brain. Postmortem studies have shown increased myelination and synaptic pruning during development, new neuron proliferation in adulthood, and reduction in somal size and neuronal fiber loss in aging. In vivo studies have confirmed regional changes in gray and white matter tissues that vary depending on the age studied and perhaps the volumetric methods used to measure age-related change. Recent cortical pattern–matching image analysis techniques have expanded our knowledge of regional changes, and exciting new results suggest that gray matter increases in specific brain regions continue into adulthood. Parsing brain changes that accompany maturation, when so many new cognitive functions are developing, and aging, when degenerative cognitive and brain changes are occurring, is complicated with in vivo studies in which the resolution needed to detect cellular changes is not available. Only by integrating the postmortem and in vivo literatures can we begin to hypothesize about the etiology of structural changes in maturation and aging that look so similar in the in vivo measures. Clearly, long-range serial studies of brain and cognitive changes (accomplishable only in vivo) and combining postmortem and imaging studies can begin to definitively answer these interesting questions. The technological advance in brain image acquisition and image analysis is staggering, and it may be that more detailed assessments of brain morphological change in vivo will be possible in the near future.

References

Anderson B, Southern BD, Powers RE. 1999. Anatomic asymmetries of the posterior superior temporal lobes: a postmortem study. Neuropsychiatry Neuropsychol Behav Neurol 12:247–54.

Ashburner J, Friston KJ. 2000. Voxel-based morphometry: the methods. Neuroimage 11:805–21.

Barkovich AJ, Kjos BO, Jackson DE Jr, Norman D. 1988. Normal maturation of the neonatal and infant brain: MR imaging at 1.5 T. Radiology 166:173–80.

Bartzokis G, Beckson M, Lu PH, Nuechterlein KH, Edwards N, Mintz J. 2001. Age-related changes in frontal and temporal lobe volumes in men: a magnetic resonance imaging study. Arch Gen Psychiatry 58:461–5.

Bartzokis G, Cummings JL, Sultzer D, Henderson VW, Nuechterlein KH, Mintz J. 2003. White matter structural integrity in healthy aging adults and patients with Alzheimer disease: a magnetic resonance imaging study. Arch Neurol 60:393–8.

Benes FM, Turtle M, Khan Y, Farol P. 1994. Myelination of a key relay zone in the hippocampal formation occurs in the human brain during childhood, adolescence, and adulthood. Arch Gen Psychiatry 51:477–84.

Blanton RE, Levitt JG, Thompson PM, Narr KL, Capetillo-Cunliffe L, Nobel A, and others. 2001. Mapping cortical asymmetry and complexity patterns in normal children. Psychiatry Res 107:29–43.

Blatter DD, Bigler ED, Gale SD, Johnson SC, Anderson CV, Burnett BM, and others. 1995. Quantitative volumetric analysis of brain MR: normative database spanning 5 decades of life. AJNR Am J Neuroradiol 16:241–51.

Brody BA, Kinney HC, Kloman AS, Gilles FH. 1987. Sequence of central nervous system myelination in human infancy. I. An autopsy study of myelination. J Neuropathol Exp Neurol 46:283–301.

Caviness VS Jr, Kennedy DN, Richelme C, Rademacher J, Filipek PA. 1996. The human brain age 7-11 years: a volumetric analysis based on magnetic resonance images. Cereb Cortex 6:726–36.

Courchesne E, Chisum HJ, Townsend J, Cowles A, Covington J, Egaas B, and others. 2000. Normal brain development and aging: quantitative analysis at in vivo MR imaging in healthy volunteers. Radiology 216:672–82.

Dekaban AS. 1978. Changes in brain weights during the span of human life: relation of brain weights to body heights and body weights. Ann Neurol 4:345–56.

Friede RL. 1989. Gross and microscopic development of the central nervous system. In: Friede RL, editor. Developmental neuropathology. 2nd ed. Berlin: Springer. p 2–20.

Fuster JM. 1997. The prefrontal cortex: anatomy, physiology, and neuropsychology of the frontal lobe. 3rd ed. New York: Lippincott-Raven.

Galaburda AM, Sanides F, Geschwind N. 1978. Human brain: cytoarchitectonic left-right asymmetries in the temporal speech region. Arch Neurol 35:812–7.

Ge Y, Grossman RI, Babb JS, Rabin ML, Mannon LJ, Kolson DL. 2002. Age-related total gray matter and white matter changes in normal adult brain. Part I: volumetric MR imaging analysis. AJNR Am J Neuroradiol 23:1327–33.

Geschwind N, Galaburda AM. 1985. Cerebral lateralization. Biological mechanisms, associations, and pathology: I. A hypothesis and a program for research. Arch Neurol 42:428–59.

Giedd JN, Blumenthal J, Jeffries NO, Castellanos FX, Liu H, Zijdenbos A, and others. 1999. Brain development during childhood and adolescence: a longitudinal MRI study. Nat Neurosci 2:861–3.

Giedd JN, Snell JW, Lange N, Rajapakse JC, Casey BJ, Kozuch PL, and others. 1996. Quantitative magnetic resonance imaging of human brain development: ages 4-18. Cereb Cortex 6:551–60.

Giedd JN, Vaituzis AC, Hamburger SD, Lange N, Rajapakse JC, Kaysen D, and others. 1996. Quantitative MRI of the temporal lobe, amygdala, and hippocampus in normal human development: ages 4-18 years. J Comp Neurol 366:223–30.

Good CD, Johnsrude IS, Ashburner J, Henson RN, Friston KJ, Frackowiak RS. 2001. A voxel-based morphometric study of ageing in 465 normal adult human brains. Neuroimage 14:21–36.

Gould E, Gross CG. 2002. Neurogenesis in adult mammals: some progress and problems. J Neurosci 22:619–23.

Hassink RI, Hiltbrunner B, Muller S, Lutschg J. 1992. Assessment of brain maturation by T2-weighted MRI. Neuropediatrics 23:72–4.

Ho KC, Roessmann U, Straumfjord JV, Monroe G. 1980. Analysis of brain weight. I. Adult brain weight in relation to sex, race, and age. Arch Pathol Lab Med 104:635–9.

Holland BA, Haas DK, Norman D, Brant-Zawadzki M, Newton TH. 1986. MRI of normal brain maturation. AJNR Am J Neuroradiol 7:201–8.

Huttenlocher PR. 1979. Synaptic density in human frontal cortex: developmental changes and effects of aging. Brain Res 163:195–205.

Huttenlocher PR, Dabholkar AS. 1997. Regional differences in synaptogenesis in human cerebral cortex. J Comp Neurol 387:167–78.

Huttenlocher PR, de Courten C. 1987. The development of synapses in striate cortex of man. Hum Neurobiol 6:1–9.

Ide A, Rodriguez E, Zaidel E, Aboitiz F. 1996. Bifurcation patterns in the human Sylvian fissure: hemispheric and sex differences. Cereb Cortex 6:717–25.

Jernigan TL, Archibald SL, Berhow MT, Sowell ER, Foster DS, Hesselink JR. 1991. Cerebral structure on MRI, part I: localization of age-related changes. Biol Psychiatry 29:55–67.

Jernigan TL, Archibald SL, Fennema-Notestine C, Gamst AC, Stout JC, Bonner J, and others. 2001. Effects of age on tissues and regions of the cerebrum and cerebellum. Neurobiol Aging 22:581–94.

Jernigan TL, Tallal P. 1990. Late childhood changes in brain morphology observable with MRI. Dev Med Child Neurol 32:379–85.

Jernigan TL, Trauner DA, Hesselink JR, Tallal PA. 1991. Maturation of human cerebrum observed in vivo during adolescence. Brain 114:2037–49.

Kertesz A, Black SE, Tokar G, Benke T, Carr T, Nicholson L. 1988. Periventricular and subcortical hyperintensities on magnetic resonance imaging. "Rims, caps, and unidentified bright objects." Arch Neurol 45:404–8.

Lange N, Giedd JN, Castellanos FX, Vaituzis AC, Rapoport JL. 1997. Variability of human brain structure size: ages 4-20 years. Psychiatry Res 74:1–12.

LeMay M, Culebras A. 1972. Human brain—morphologic differences in the hemispheres demonstrable by carotid arteriography. N Engl J Med 287:168–70.

MacDonald D, Avis D, Evans A. 1994. Multiple surface identification and matching in magnetic resonance images. Proceedings Visualization in Biomedical Computing 2359:160–9.

Marner L, Nyengaard JR, Tang Y, Pakkenberg B. 2003. Marked loss of myelinated nerve fibers in the human brain with age. J Comp Neurol 462:144–52.

Narr KL, Thompson PM, Sharma T, Moussai J, Zoumalan C, Rayman J, and others. 2001. Three-dimensional mapping of gyral shape and cortical surface asymmetries in schizophrenia: gender effects. Am J Psychiatry 158:244–55.

Pakkenberg B, Gundersen HJ. 1997. Neocortical neuron number in humans: effect of sex and age. J Comp Neurol 384:312–20.

Paus T, Zijdenbos A, Worsley K, Collins DL, Blumenthal J, Giedd JN, and others. 1999. Structural maturation of neural pathways in children and adolescents: in vivo study. Science 283:1908–11.

Penhune VB, Zatorre RJ, MacDonald JD, Evans AC. 1996. Interhemispheric anatomical differences in human primary auditory cortex: probabilistic mapping and volume measurement from magnetic resonance scans. Cereb Cortex 6:661–72.

Pfefferbaum A, Mathalon DH, Sullivan EV, Rawles JM, Zipursky RB, Lim KO. 1994. A quantitative magnetic resonance imaging study of changes in brain morphology from infancy to late adulthood. Arch Neurol 51:874–87.

Raz N, Gunning FM, Head D, Dupuis JH, McQuain J, Briggs SD, and others. 1997. Selective aging of the human cerebral cortex observed in vivo: differential vulnerability of the prefrontal gray matter. Cereb Cortex 7:268–282.

Reiss AL, Abrams MT, Singer HS, Ross JL, Denckla MB. 1996. Brain development, gender and IQ in children: a volumetric imaging study. Brain 119:1763–74.

Resnick SM, Goldszal AF, Davatzikos C, Golski S, Kraut MA, Metter EJ, and others. 2000. One-year age changes in MRI brain volumes in older adults. Cereb Cortex 10:464–72.

Salat DH, Kaye JA, Janowsky JS. 2001. Selective preservation and degeneration within the prefrontal cortex in aging and Alzheimer disease. Arch Neurol 58:1403–8.

Sowell ER, Delis D, Stiles J, Jernigan TL. 2001. Improved memory functioning and frontal lobe maturation between childhood and adolescence: a structural MRI study. J Int Neuropsychol Soc 7:312–22.

Sowell ER, Jernigan TL. 1998. Further MRI evidence of late brain maturation: limbic volume increases and changing asymmetries during childhood and adolescence. Dev Neuropsychol 14:599–617.

Sowell ER, Peterson BS, Thompson PM, Welcome SE, Henkenius AL, Toga AW. 2003. Mapping cortical change across the human life span. Nat Neurosci 6:309–15.

Sowell ER, Thompson PM, Holmes CJ, Batth R, Jernigan TL, Toga AW. 1999. Localizing age-related changes in brain structure between childhood and adolescence using statistical parametric mapping. Neuroimage 9:587–97.

Sowell ER, Thompson PM, Holmes CJ, Jernigan TL, Toga AW. 1999. In vivo evidence for post-adolescent brain maturation in frontal and striatal regions. Nat Neurosci 2:859–61.

Sowell ER, Thompson PM, Peterson BS, Mattson SN, Welcome SE, Henkenius AL, and others. 2002. Mapping cortical gray matter asymmetry patterns in adolescents with heavy prenatal alcohol exposure. Neuroimage 17:1807–19.

Sowell ER, Thompson PM, Rex D, Kornsand D, Tessner KD, Jernigan TL, and others. 2002. Mapping sulcal pattern asymmetry and local cortical surface gray matter distribution in vivo: maturation in peri-sylvian cortices. Cereb Cortex 12:17–26.

Sowell ER, Thompson PM, Tessner KD, Toga AW. 2001. Mapping continued brain growth and gray matter density reduction in dorsal frontal cortex: inverse relationships during postadolescent brain maturation. J Neurosci 21:8819–29.

Sowell ER, Trauner DA, Gamst A, Jernigan TL. 2002. Development of cortical and subcortical brain structures in childhood and adolescence: a structural MRI study. Dev Med Child Neurol 44:4–16.

Terry RD, DeTeresa R, Hansen LA. 1987. Neocortical cell counts in normal human adult aging. Ann Neurol 21:530–9.

Thompson PM, Cannon TD, Narr KL, van Erp T, Poutanen VP, Huttunen M, and others. 2001. Genetic influences on brain structure. Nat Neurosci 4:1253–8.

Thompson PM, Giedd JN, Woods RP, MacDonald D, Evans AC, Toga AW. 2000. Growth patterns in the developing brain detected by using continuum mechanical tensor maps. Nature 404:190–3.

Thompson PM, Hayashi KM, de Zubicaray G, Janke AL, Rose SE, Semple J, and others. 2003. Dynamics of gray matter loss in Alzheimer's disease. J Neurosci 23:994–1005.

Thompson PM, Hayashi KM, de Zubicaray G, Janke AL, Sowell ER, Rose SE, and others. 2003. Dynamic mapping of Alzheimer's disease. In: Proceedings of the 19th Colloque Médecine et Recherche, IPSEN Foundation. New York: Springer-Verlag.

Thompson PM, Mega MS, Narr KL, Sowell ER, Blanton RE, Toga AW. 2000. Brain image analysis and atlas construction. In: Fitzpatrick M, Sonka M, editors. SPIE handbook on medical image analysis. Bellingham (WA): Society of Photo-optical Instrumentation Engineers Press.

Thompson PM, Mega MS, Vidal C, Rapoport JL, Toga AW. 2001. Detecting disease-specific patterns of brain structure using cortical pattern matching and a population-based probabilistic brain atlas. In: Insana M, Leahy R, editors. IEEE conference on information processing in medical imaging (IPMI). New York: Springer-Verlag. p 488–501.

Thompson PM, Mega MS, Woods RP, Zoumalan CI, Lindshield CJ, Blanton RE, and others. 2001. Cortical change in Alzheimer's disease detected with a disease-specific population-based brain atlas. Cereb Cortex 11:1–16.

Thompson PM, Moussai J, Zohoori S, Goldkorn A, Khan AA, Mega MS, and others. 1998. Cortical variability and asymmetry in normal aging and Alzheimer's disease. Cereb Cortex 8:492–509.

Thompson PM, Toga AW. 1997. Detection, visualization and animation of abnormal anatomic structure with a deformable probabilistic brain atlas based on random vector field transformations. Med Image Anal 1:271–94.

Thompson PM, Toga AW. 2002. A framework for computational anatomy. Computing and Visualization in Science 5:1–12.

Thompson PM, Vidal C, Giedd JN, Gochman P, Blumenthal J, Nicolson R, and others. 2001. Mapping adolescent brain change reveals dynamic wave of accelerated gray matter loss in very early-onset schizophrenia. Proc Natl Acad Sci U S A 98:11650–5.

Toga AW, Thompson PM. 2003. Mapping brain asymmetry. Nat Rev Neurosci 4:37–48.

Watkins KE, Paus T, Lerch JP, Zijdenbos A, Collins DL, Neelin P, and others. 2001. Structural asymmetries in the human brain: a voxel-based statistical analysis of 142 MRI scans. Cereb Cortex 11:868–77.

Witelson SF, Pallie W. 1973. Left hemisphere specialization for language in the newborn: neuroanatomical evidence of asymmetry. Brain 96:641–6.

Yakovlev PI, Lecours AR. 1967. The myelogenetic cycles of regional maturation of the brain. In: Minkowski A, editor. Regional development of the brain in early life. Oxford (UK): Blackwell Scientific. p 3–70.